

Chapter 1

Introduction

1.1 Significance

Signal transduction is a recurring theme of cell biology. Extra-cellular ligand binding to membrane spanning receptor proteins is followed by specific cellular responses, typically revolving around control of gene expression, progression through the cell cycle, protein redistribution, cell adhesion and migration or metabolism. Protein-protein interactions play crucial roles in mediating these extra-cellular signals to specific biological responses. Modular intra-cellular proteins are involved in these processes, in either catalytic or adaptor type roles. A common feature of these modular proteins is that they contain non-catalytic homology domains, like the Src Homology 2 and 3 domains (SH2 and SH3). SH2 domains recognise phosphotyrosine motifs¹ while SH3 domains recognise short proline-rich peptide sequences.¹⁻³ Since deregulated signalling pathways form the basis of a range of human diseases, there has been extensive research into the structure and functions of the SH2 and SH3 domains, and both of these domains have been appealing targets for the development of potential therapeutics. In the case of the SH2 domains, examples of non-peptide ligands have been reported,⁴⁻⁶ however the success of studies targeted towards the SH3 domains has been limited to ligands without deviation from the traditional proline-rich peptide core. Prior to the commencement of this PhD project, no examples of entirely non-peptide ligands for the SH3 domains had been reported.

In this PhD thesis, a comprehensive study into the use of a well-known class of heterocyclic compound, as 'leads' for the development of small molecule ligands for the SH3 domains will be presented. Prior to the commencement of this work, compounds of this class had been identified as ligands, with weak to moderate affinity, for the Tec SH3 domain. In order to place this work into context, the structure, ligand binding properties, and then the relevance of the SH3 domains as targets for drug design will first be presented. Relevant aspects of the 'drug design cycle' will also be discussed. Then, the 'lead' small molecule ligands for the Tec SH3 domain will be introduced. Finally, an outline for the planned use of the 'leads' during this work is presented, followed by the results in the following chapters.

1.2 The SH3 Domains

1.2.1 SH3 domain structure

The SH3 domains are small protein units (55-70 residues). As at November 2004, there were at least 145 entries in the Protein Data Bank (PDB) of structures containing an SH3 domain sequence (SMART search⁷). The conserved fold (Figure 1-1) consists of five anti-parallel β -strands (termed β A to β E), that organise into two perpendicular β -sheets, β I and a larger β II, to form a β -barrel. The β I sheet consists of strands β A, part of β B and β E, and the β II sheet consists of the remainder of the β B strand and the β C and β D strands. There is a kink in the polypeptide chain of the β B strand that allows it to participate in both sheets. Linking strands β A and β B is the long 'RT' (arginine-threonine) loop (the length of which can vary considerably between SH3 domains), and linking strands β B to β C is the 'n-Src' loop.⁸ In addition, there is a 3_{10} helix in the region connecting the β D and β E strands. This overall fold results in the conserved, mostly hydrophobic residues being brought close together to form a ligand binding surface. Three pockets exist on the binding surface.^{9,10} Two of these pockets are termed the 'LP' (leucine-proline) pockets and constitute shallow grooves approximately 25Å long and 10Å wide,¹⁰ which together accommodate two consecutive leucine-proline dipeptide segments from the ligand. The third pocket, often referred to as the 'specificity pocket' consists of the regions flanked by the RT and n-Src loops, and frequently contains an acidic residue that accommodates a conserved basic residue of the ligand by forming a salt bridge (Figure 1-2).

1.2.2 SH3 domain ligands: early discoveries

A first step towards understanding SH3 domain ligands was made when the products of a cDNA expression library from mouse pre-B cells were screened for binding to the SH3 domain of Abl.¹¹ This led to the isolation of 3BP-1 as an Abl SH3 binder, however 3BP-1 was also able to bind other SH3 domains with varying affinities. As an extension of this work, a combination of deletion and alanine mutagenesis experiments on 3BP-1 and comparison with 3BP-2 and similar sequences identified through database searching, identified the sequence XPXXPPP Ψ XP (where P is proline, X is any other amino acid except cysteine, and Ψ a hydrophobic residue frequently leucine) as a consensus for SH3 binding.¹² The underlined prolines were shown to be essential for binding of 3BP-1 to the Abl SH3 domain, whilst when the X residue (proline in 3BP-1) was replaced with alanine, weaker binding of the

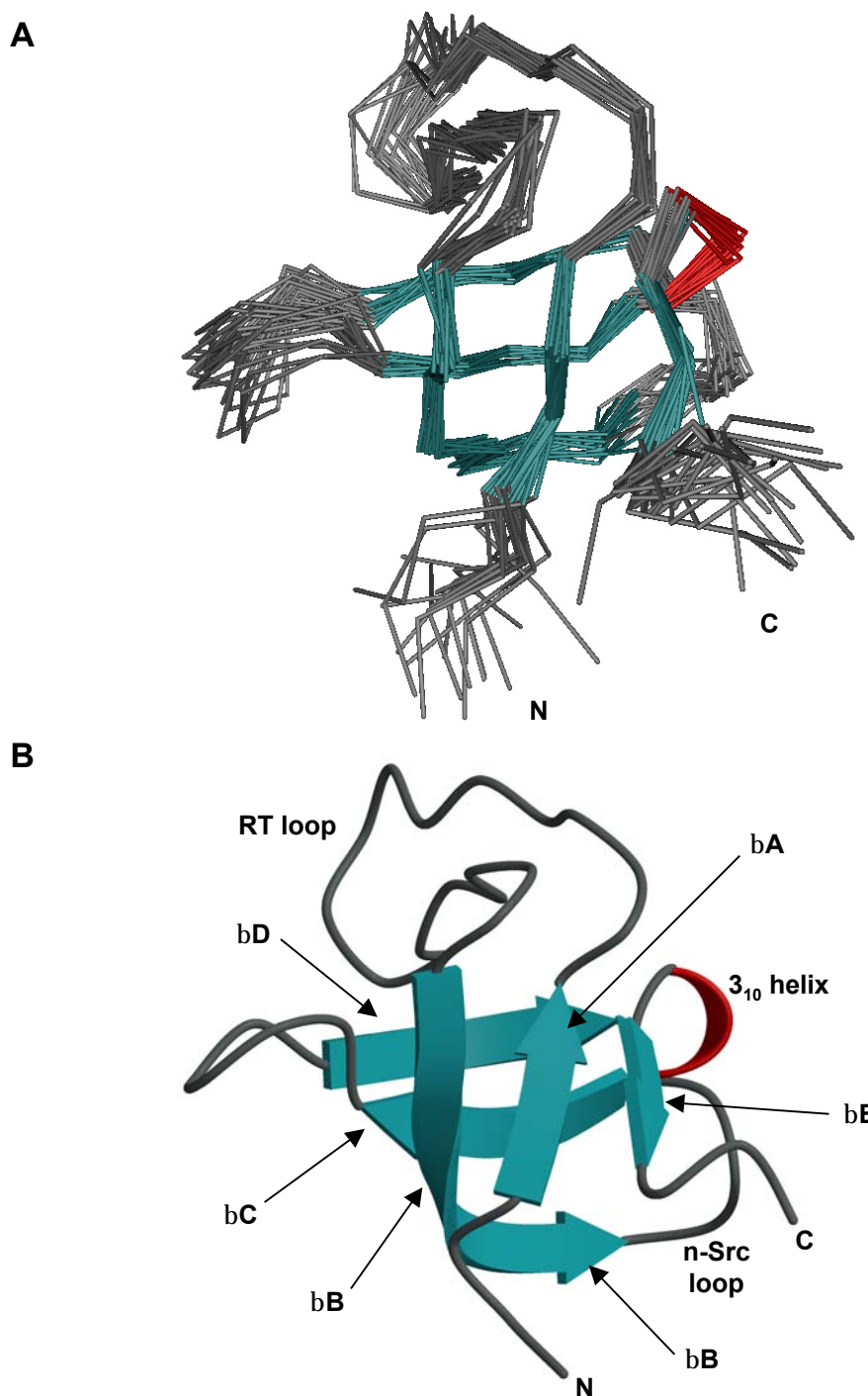


Figure 1-1: The structure of the mouse Tec SH3 domain, determined using NMR spectroscopy.¹³ (PDB Entry 1GL5.pdb) (A) Ensemble of the twenty final structures. The regions in aqua represent β -strands, while the region in red represents the 3_{10} helix. (B) Cartoon representation of 'Model 1' of the 20 structures, with the β -sheet system illustrated, along with the 3_{10} helix, and the n-Src and the RT loops.

ligand was observed. Biased combinatorial peptide libraries of the form XXXPPXPXX have since been prepared (again where P is proline and X is any other residue except cysteine).¹⁴ This work identified a series of novel ligands for the SH3 domain of PI3-K with affinities in the 7 to 30 μ M range. On comparison of the sequences of the isolated ligands, the peptides

could be placed into two classes: one that contained an N-terminal arginine residue, and another that contained a C-terminal arginine residue. It was proposed that these ligands might bind in different orientations. NMR spectroscopy was subsequently used to determine the structures of the Src SH3 domain in complex with two proline-rich peptides, one from each of the proposed classes, and two binding orientations were confirmed,⁹ where the N and C termini of the two classes were in opposite directions. The peptides both bound in a left-handed poly-proline type-2 helix (PPII), however the direction of the binding was determined by a salt bridge between a terminal basic residue on the ligand and a conserved acidic residue of the SH3 domain. It was also found that residues at positions 3, 4, 6 and 7 of both peptides intercalate with the ligand binding site and the relative positions of proline and non-proline residues were exchanged between the two complexes. It is now accepted that

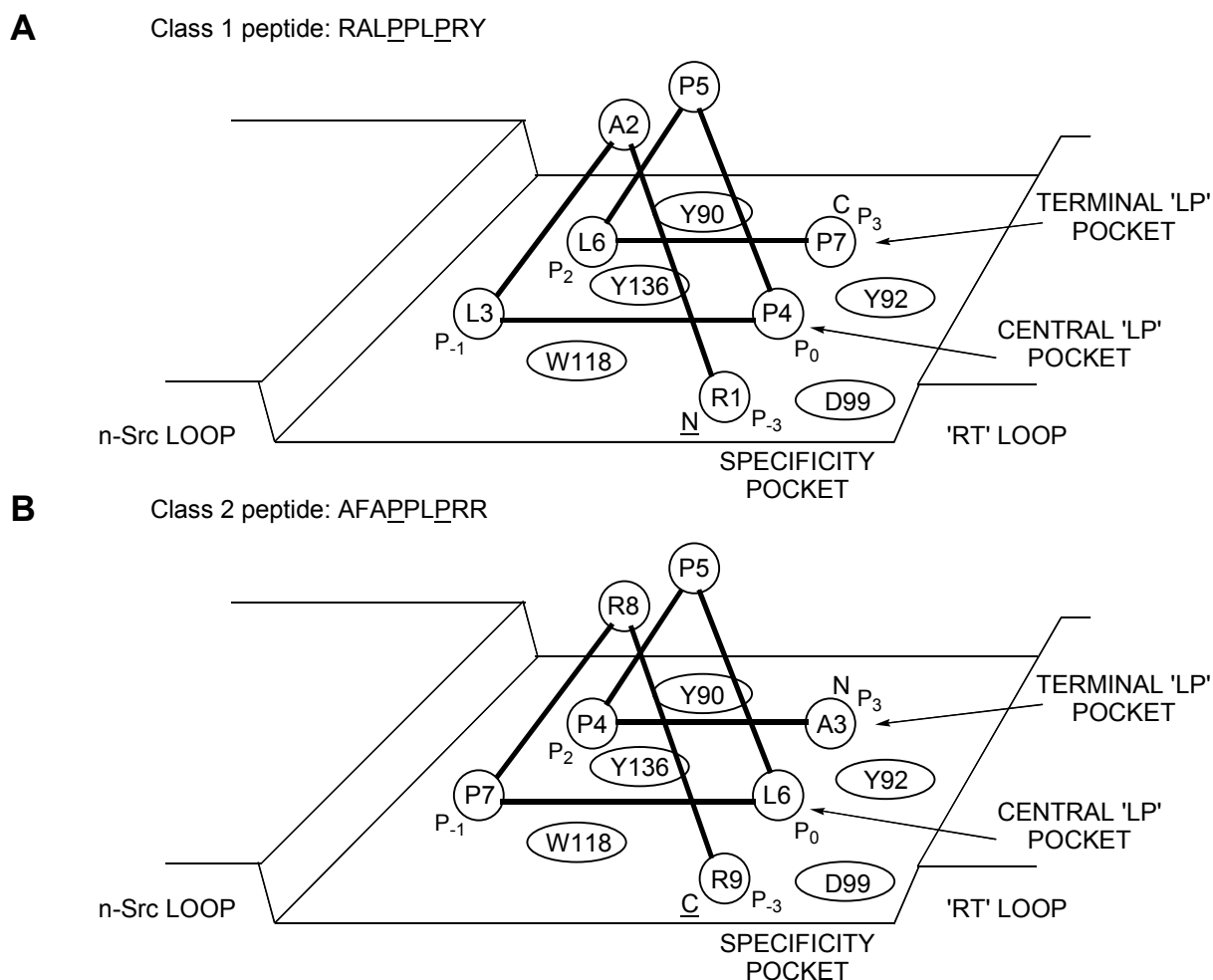


Figure 1-2: Schematic representation of the interaction between the Class 1 and Class 2 proline-rich peptides for the Src SH3 domain. (A) Class 1 proline-rich peptide ligand RLP2. (B) Class 2 proline-rich peptide ligand PLR1 (B). Important binding positions are denoted with P, where P₋₁/P₀ constitutes the central 'leucine-proline' (LP) pocket, P₂/P₃ the terminal LP pocket, and P₋₃ the specificity pocket. Notice the relative positions of the P4 and P7 residues between classes. Mutagenesis studies have also revealed, that proline P5 plays an important "scaffolding" rather than "contacting" role, which stabilises ligand binding.⁹ (Adapted from Figure 3 in Dalgarno¹⁵ and Figure 3 in Feng⁹)

there are two classes of SH3 peptide ligands denoted Class 1 (R/KXXPPXXP) and Class 2 (XPXXPR/K) as illustrated in Figure 1-2 (using Class 1 and 2 peptides for the Src SH3 domain as an example). This model has since successfully been used to predict the binding of two proline-rich regions of Sos as Class 2 orientations when bound to the two SH3 domains of Grb2.¹⁶

The consensus sequence for proline-rich peptide ligands is often expressed simply as PXXP, however sequences of the nature XPpXP where P is proline, p is preferred as proline, and X is leucine or another hydrophobic residue, are common for many SH3 binding peptides.^{10,17-21} The underlined prolines are essential for contacting the LP pocket of the SH3 domain, whilst the lower case proline plays a scaffolding role, by assisting to maintain the poly-proline type 2 helix.

1.2.3 Recent developments with SH3 ligands

1.2.3.1 Proline-rich peptides containing non-peptide binding elements

Since the early studies into the SH3 domain ligands, different approaches have been used to identify novel SH3 ligands. For example, using combinatorial chemistry with a range of small-molecule monomers in conjunction with a biasing PLPPLP element lead to the identification of Src SH3 domain ligands with non-peptide elements with low micromolar affinities.¹⁸ NMR spectroscopy was used to determine the structure of some of these novel Src SH3-ligand complexes and illustrated that the non-peptide binding elements were interacting with the specificity pocket of the SH3 domain.²² Further studies using the same approach involved designing a new library of non-natural amino acid monomers to attach to the biasing element that targeted the specificity pocket and identified novel ligands with improved affinity for the Src SH3 domain.¹⁹ Using a similar approach, but instead directing the biasing element to the specificity and central LP di-peptide pockets, the same researchers incorporated non-peptide binding elements that were targeted to the second LP pocket as a means of investigating the binding preferences at this site.¹⁰ Novel ligands were subsequently identified that had non-peptide binding elements targeted to the terminal LP pocket with low micromolar affinities, illustrating that non-peptide elements could replace the prolines that would normally fill this pocket. A chimeric peptide was prepared consisting of the optimised non-peptide elements targeted to the specificity pocket and the outer LP pocket, with the biasing sequence, proline and leucine residues, targeting the central LP pocket as a linker (Figure 1-3). This afforded a Src SH3 ligand that bound with comparable affinity to the previously defined ligands.¹⁰

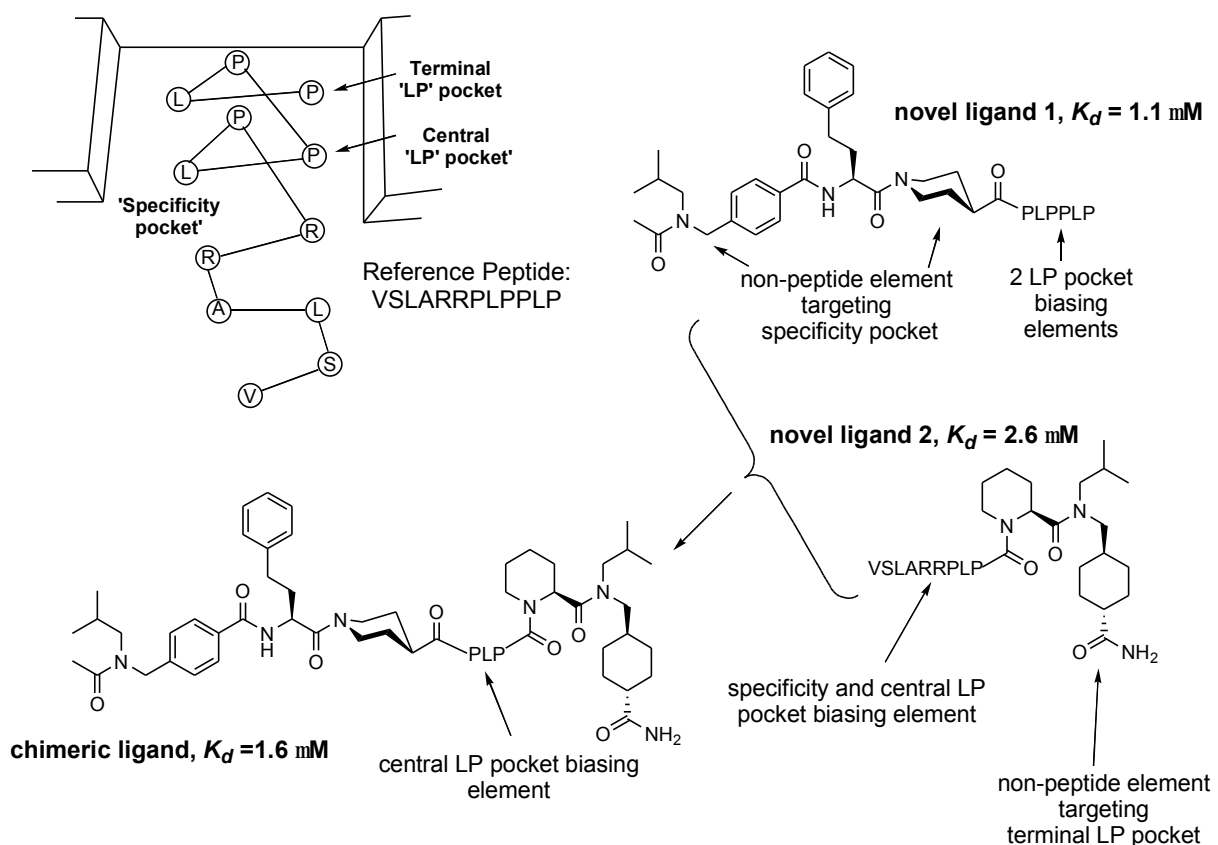


Figure 1-3: A summary of the work in the Schreiber^{10,18,19,22} laboratory, which identified SH3 ligands with extensive non-peptide deviation from the traditional proline rich core.

1.2.3.2 Peptoid ligands: use of non-natural amino acids

Perhaps the most elegant studies towards development of higher affinity SH3 ligands comes from the laboratory of Lim.^{23,24} This work revolves around the idea that SH3 domains recognise proline residues because proline is the only naturally occurring amino acid that is substituted on the backbone nitrogen atom.^{23,24} Key 'proline site' residues from the Sem5 proline-rich peptide ligand (YEVPVPPVPPRRR) were replaced with either alanine ($C\alpha$ -substituted) or sarcosine (N -substituted, no $C\alpha$ -substitution) (Figure 1-4), to identify crucial positions along the proline rich core. Two positions (P_{-1} and P_2) were identified to specifically require N -substitution (sarcosine tolerant, alanine intolerant), and the consecutive site to P_{-1} (P_0), was found to require $C\alpha$ -substitution (sarcosine intolerant, alanine tolerant). Hence a series of non-natural N -substituted amino acids were put in place of proline residues at the key P_{-1} and P_2 sites in the Sem5 proline-rich peptide, and were tested for binding to the SH3 domains of Sem5, Crk, Grb2 and Src, all of which share a preference for a PXXPXR consensus. A number of these peptides (or 'peptoids') were able to bind the SH3 domains with affinities as good or better than the natural proline-rich peptides.²⁴ One peptide bound the SH3 domain of Grb2 with $K_d = 40$ nM, more than one hundred-fold higher affinity than the wild type peptide, illustrating a remarkable improvement in binding strength.

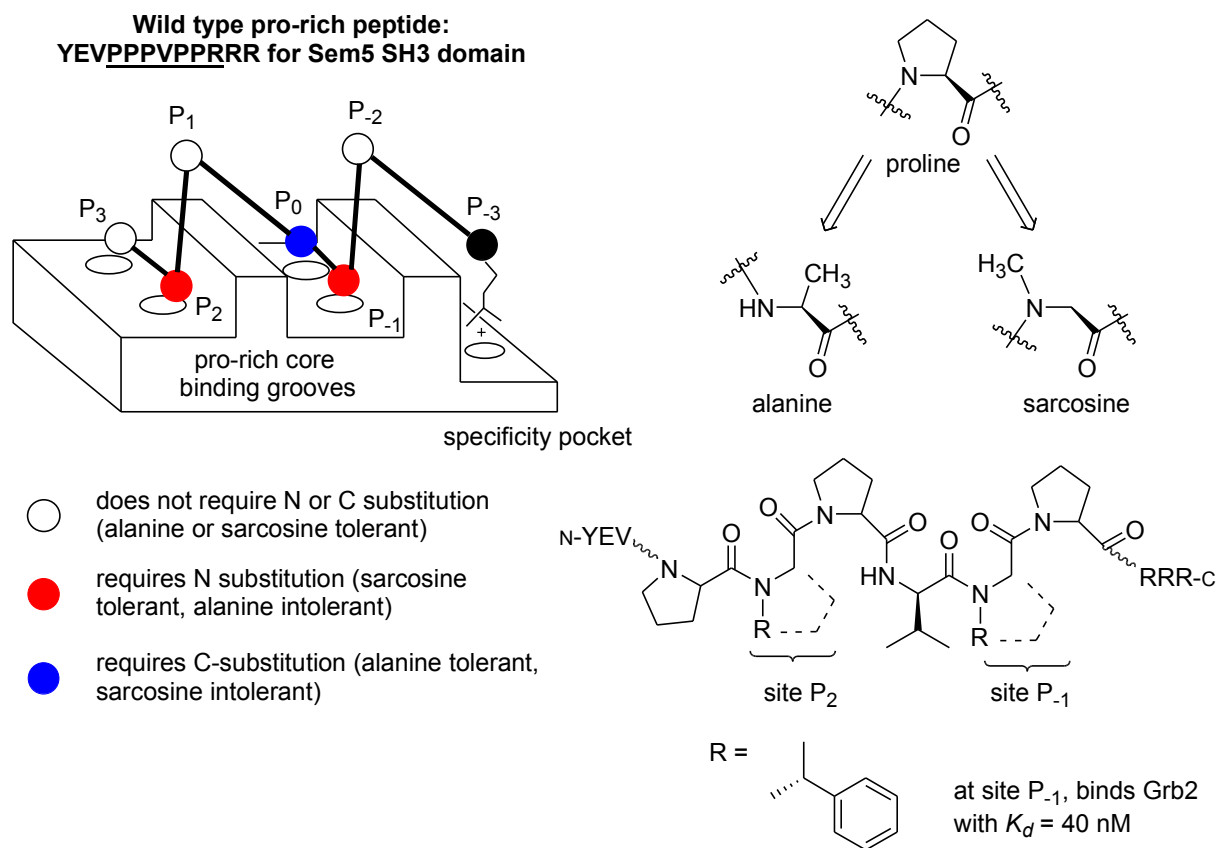
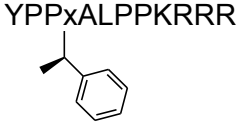
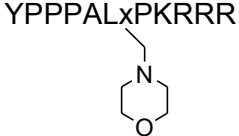
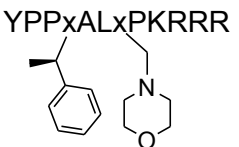


Figure 1-4: A summary of the pioneering work of Lim which investigated the nitrogen substitution requirements in proline rich ligands, and subsequently led to the first nanomolar SH3 ligand.²⁴

Further research involving the above strategy focused on varying the side chains of the *N*-substituents with the aim of ‘fine tuning’ an SH3 ligand for a particular domain.²³ Some peptoids were prepared with both of the crucial P₂ and P₋₁ prolines replaced with non-natural residues that could bind the SH3 domains, however no major improvements in specificity were initially obtained. Domain specific peptides were next synthesised with flanking sequences about the proline rich core specific to either the Crk or Src SH3 domains. Variants of the domain specific peptides were prepared with either one or two of the crucial P₂ and P₋₁ prolines replaced with non-natural *N*-substituted amino acids (Table 1-1). One particular peptoid was able to bind to the SH3 domain of Crk with a K_d of 8 nM, whilst the same peptoid bound the N-Grb2 and Src SH3 domains with $K_d = 13.7$ and 45.6 μ M respectively, illustrating a very high degree of selectivity. Another peptoid was able to bind to Crk with an affinity of 1.98 μ M, but no binding to Src or N-Grb2 was observed, illustrating that a cross reactive peptide could be tuned to a particular domain.

Table 1-1: Dissociation constants for some peptoids derived from a Crk SH3 domain specific peptide, illustrating how a particular SH3 ligand can be 'tuned' for a particular domain (Adapted from Table 1 in Lim.²³).

Crk Domain Specific Peptoids	N-Grb2 K_d (mM)	Crk K_d (mM)	Src K_d (mM)
YPPPALPPKRRR (reference)	24.9	0.02	86.8
YPPxALPPKRRR 	13.7	0.008	45.6
YPPPALxPKRRR 	>904	0.5	No binding
YPPxALxPKRRR 	No binding	1.98	No binding

1.2.3.3 UCS15A: a non-peptide SH3/proline-rich peptide inhibitor

More recently, screens of microbial products led to the discovery of the non-peptide compound UCS15A (Figure 1-5), as a non-kinase inhibitor of Src mediated signal transduction.²⁵ Subsequently, it was determined that this inhibition was mediated by the ability of UCS15A to disrupt the interaction between the Src SH3 domain and Sam68, following immunoprecipitation experiments using HCT116 cells that had been treated with UCS15A.²⁶ Furthermore, a similar approach indicated that the Sam68/Grb2-SH3, Sam68/PLC γ -SH3, ZO1/cortactin-SH3 and Sos/Grb2-SH3 interactions were also disrupted by UCS15A, however SH2 domain mediated interactions were not inhibited by UCS15A. At this stage it was unclear whether the mode of this inhibition was mediated by the SH3 domain, or by the proline-rich peptide component of the complexes. To address this, the Src SH3 domain was treated with UCS15A prior to incubation with Sam68, and conversely, Sam68 was treated with UCS15A prior to incubation with the Src SH3 domain. Of these two scenarios, the immunoprecipitation experiments revealed that only the Sam68/UCS15A pre-treated protein was able to inhibit complex formation with the Src SH3 domain. This result was also reproduced in experiments where the excess UCS15A was removed after the pre-treatment of Sam68, by ultrafiltration. These results suggested that the mechanism of the UCS15A inhibition was probably mediated by interaction of UCS15A with the proline-rich

peptide. Furthermore, UCS15A could not disrupt a pre-formed Sam68/Src SH3 complex *in vitro*. This suggested that UCS15A was unable to disrupt the pre-existing complex, but instead only inhibit its formation.

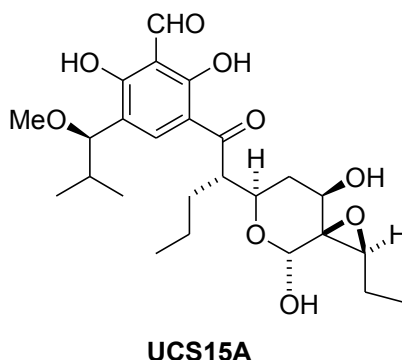


Figure 1-5: Structure of UCS15A, a natural product identified as an inhibitor of proline-rich peptide/SH3 mediated protein-protein interactions, however, the mechanism of this inhibition was shown to be mediated by binding of UCS15A to the proline-rich peptide, not the SH3 domain.^{26,27}

An elaboration of this work, involving the synthesis of a range of derivatives of UCS15A, led to the discovery of derivatives with improved potency (with best $IC_{50} < 20 \mu M$),²⁷ and provided some basic structure activity information about the interaction. However, the mechanism of the binding of UCS15A and the derivatives with proline-rich peptides remains unclear. No further developments on the use of UCS15A or related derivatives as SH3/proline-rich peptide inhibitors have since been reported.

1.2.4 Biology of the SH3 domains

SH3 domains frequently feature in enzymes that are involved in cell signalling pathways, such as the non-transmembrane protein tyrosine kinases (PTKs), like the Src or Tec family members. Alternatively, these signalling pathways frequently involve SH3 containing adaptor proteins such as Grb2, Shc and the p85 unit of PI3K. These pathways couple membrane spanning activated receptors to downstream effectors. Examples of each of these SH3 containing proteins are discussed below.

1.2.4.1 The Tec family of non-transmembrane Protein Tyrosine Kinases (PTKs)

Tec (Figure 1-6) consists of the five members Tec, Btk, Itk/Tsk/Emt, Rlk/Txk and Bmx, and is the second largest family of non-transmembrane PTKs.²⁸ Many members of the Tec family are expressed in hematopoietic tissues and are thought to play important roles in growth and differentiation processes in the blood.²⁹ Although there is a lack of clearly identified

substrates of Tec, there is evidence to suggest that it is involved downstream of certain receptor proteins, including gp130³⁰ and c-kit,³¹ and roles in T-cell signalling³² have also been implicated. More recently, Tec family members have also been implicated in regulation of the actin cytoskeleton (reviewed in Cannons³³).

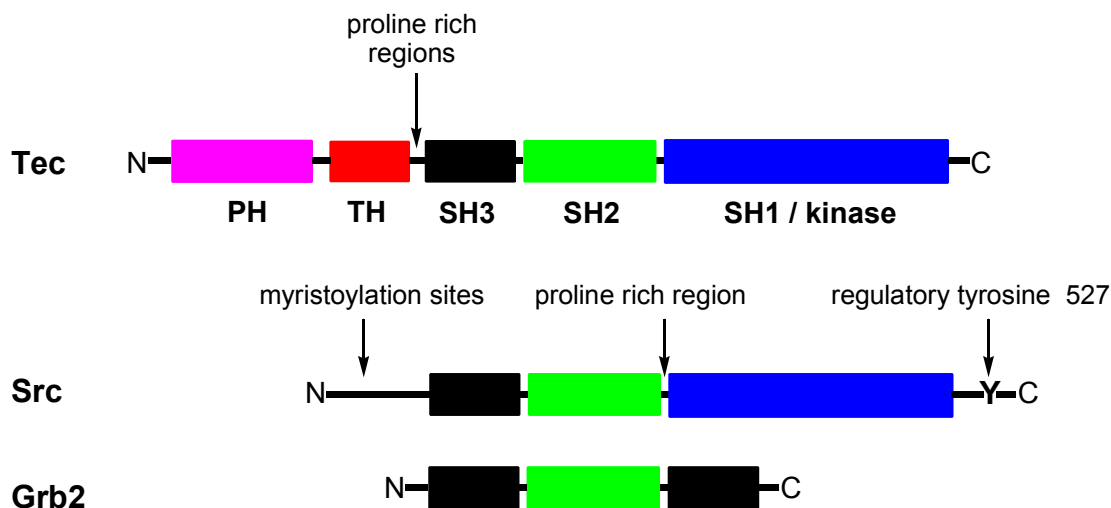


Figure 1-6: Examples of SH3 containing proteins: schematic representation of the Tec and Src family protein tyrosine kinases and the Grb-2 adaptor protein for comparison.

The Tec family proteins, ranging in size from 62-77 kDa, consist of (N to C) the Pleckstrin Homology (PH) domain, Tec Homology Domain, a proline-rich region, the Src Homology domains 3 and 2, (SH3 and SH2), followed by the SH1 or kinase domain (Figure 1-6). Apart from the absence of the PH and TH domains in the Src family kinases, the Tec family PTKs have structural similarities to the Src family kinases (compared in Figure 1-6). However there are substantial differences in the way that the two enzymes are regulated. The Tec family kinases lack the C-terminal tyrosine residue that when phosphorylated binds to the SH2 domain of Src in an intramolecular fashion. However, Tec has a region in between the TH and SH3 domains that is rich in proline residues, and these constitute SH3 domain ligands which can interact in an inter- and intra-molecular fashion. Specifically, the proline rich region of Itk has been shown to bind intra-molecularly to its own SH3 domain *in vitro*, leaving the phospho-tyrosine binding site of the SH2 domain exposed, but overall leaving the enzyme in a closed conformation.³⁴ Introduction of SH2 and competing SH3 ligands, opens up the enzyme. The Tec IV protein contains two distinct SH3 ligands within its proline-rich region.¹³ One of these ligands is able to bind to the SH3 domain in a low affinity intra-molecular fashion, whilst the second ligand binds in a higher affinity inter-molecular fashion, which is likely to be important for targeting and enzyme activation.¹³

1.2.4.2 The Grb2 adaptor protein

Grb2 is an adaptor protein with no catalytic function that contains two SH3 domains and one SH2 domain (Figure 1-6). A well characterised role of Grb2 is in the Ras/MAPK signalling pathway that is involved in cell division, differentiation and cytoskeletal reorganisation in response to growth factor receptor activation (reviewed in Garbay¹). As illustrated in Figure 1-7 below, extra-cellular binding of growth factors to membrane spanning receptors, results in auto-phosphorylation on a tyrosine residue on the intra-cellular domain of the receptor, which leads to recruitment of Grb2 to the membrane via its SH2 domain. This allows binding of Sos to the SH3 domain of Grb2 mediated by the proline-rich regions of Sos, and Sos subsequently mediates the exchange of a GDP molecule from an inactive Ras, for a GTP resulting in formation of the activated Ras. The active Ras then recruits Raf, and triggers a cascade of further cell signalling events, involving MAP-kinases, that typically lead to cellular growth or differentiation.

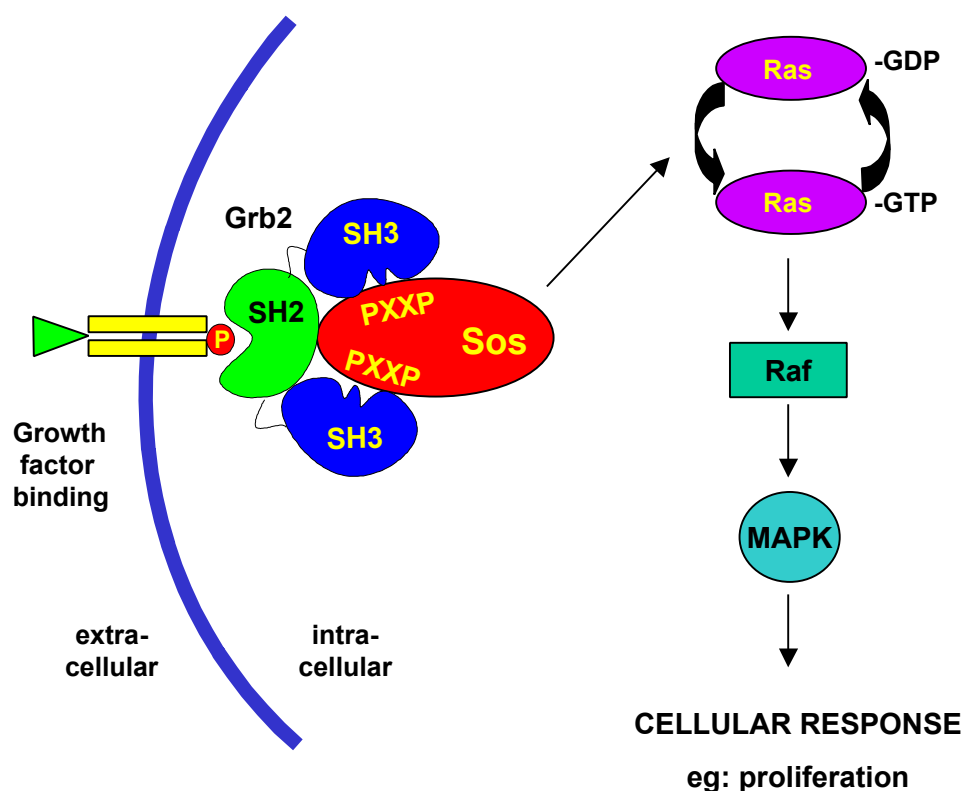


Figure 1-7: Cartoon diagram of the Grb2/Sos/MAPK signalling pathway, resulting from extra-cellular growth factor binding. Adapted from Figure 1 in Vidal.¹

1.2.4.3 SH3 domains as targets for therapeutic development

SH3 containing proteins are frequently found in deregulated signalling pathways including oncogenic pp60c-Src (involved in breast cancer), Nck (possibly involved in tumour metastasis) and Grb2 (human cancers) (reviewed in Garbay¹ and Dalgarno¹⁵). Grb2 (Figure

1-6), although not an oncogenic protein, is likely to be involved in several protein complexes associated with human cancers.¹ For example, over production of Grb2 has been implicated in breast cancer in conjunction with both HER2 production and an increase in Grb2/Sos complex formation (in a similar context to that illustrated in Figure 1-7). High expression of the human Tec gene was identified in three patients with myelodysplastic syndrome, however a clear connection between this condition and over expression of the Tec gene has yet to be proven.³⁵ Bruton's tyrosine kinase (Btk), another member of the Tec family, has also been implicated as a deficient enzyme in X-linked agammaglobulinemia (XLA).³⁶

As SH3 containing proteins have been implicated in a number of deregulated signalling pathways, they are considered as valuable targets for the design of anti-proliferative agents. For example, studies of Ras signalling pathways in HER-2 transformed cells with a mutant form of Grb2 that had either N or C terminal SH3 domain deletions, inhibited Shc/Grb2/Sos complex formation and reversed the transformed phenotype caused by a mutant activated form of rat HER-2.³⁷ Similarly, studies involving a form of Sos with mutations in the proline-rich regions again prevented the formation of a functional Shc/Grb2/Sos complex and hence phosphorylation of MAP kinases ERK1 and ERK2.³⁸ Thus ligands targeted to SH3 domains have the potential to intervene in such signalling pathways.

Although nanomolar affinity 'peptoid' SH3 ligands have been developed (described in Section 1.2.3.2), these ligands are too large and peptide-like to be useful compounds for therapeutic use. Specifically, there are often problems with delivery of such compounds into the cell, and coupling of peptide ligands to cell permeable peptides³⁹ is often required. Therefore, there is clearly a need to develop high affinity, highly specific non-peptide compounds as SH3 ligands, with improved membrane permeability.

1.3 Strategies in drug discovery

One major challenge faced by the pharmaceutical industry is the identification of lead molecules as candidates for drug development. Traditional methods involve screening a target against large libraries of commercially available compounds or natural product molecules (high through put screening or HTS). However, several problems are associated with this strategy. HTS can be very costly and laborious. To screen such a large quantity of compounds requires large amounts of protein (or other reagents) and personnel (although automated methods have been developed). Due to the randomness of the approach, a large quantity of compounds (typically > 100, 000) must be screened to maximise the probability of a lead being identified. Depending on the screening method used, HTS may be done by

pooling several compounds together and then screening them against the target. If there is evidence of an active compound, one must then go back and identify which compound(s) out of the pool is active. Where HTS does identify a potential new class of compounds for drug use, the class may not lead to a practical range of synthetically viable compounds without compromising desirable aspects of solubility, bioavailability or toxicity.⁴⁰ Likewise, identification of natural products as lead compounds may not always be ideal from the point of view of synthetic accessibility.⁴⁰

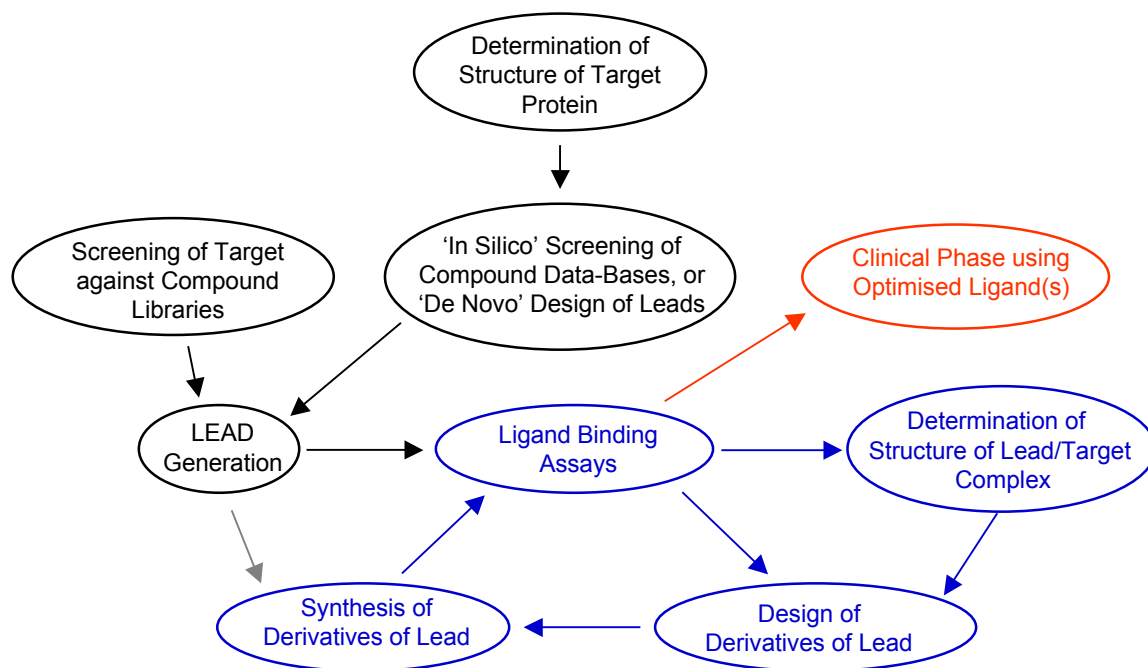


Figure 1-8: Aspects of the 'Drug Design Cycle'. The three different colours used represent three different phases of the development process. The first phase, (black) is primarily concerned with identification of a lead compound for drug development, the second phase (blue) is primarily concerned with the optimisation of binding affinity of the lead, whilst the final phase (red), is concerned with confirming the desired biological response, in conjunction with studying important pharmacological properties, such as toxicity, stability and cell delivery.

When a lead is identified, several more cycles of synthesis usually follow using the lead molecule so that its structure can be refined to optimise binding affinity. Where a structural approach is being used in the design strategy, a 3D structure of the ligand/target protein complex may be obtained to assist with characterising the binding mode. Once a high affinity ligand has been identified (typically with affinity in the nanomolar range or lower), the compound must satisfy further testing where factors such as toxicity, bioavailability, and resistance are investigated. Typically a drug may take 15 years and cost \$350-500 million to reach the market.⁴¹ Aspects of the 'drug design cycle' are illustrated in Figure 1-8 above.

1.3.1 Computational methods in drug design

With the amount of 3D information on bio-molecules presently available, the use of computational methods in drug development is becoming more important. Computational methods are now playing an increasing role in assisting with aspects of the 'drug design cycle' (Figure 1-8), particularly at the lead generation phase.⁴² For example, a series of compounds for a target can be designed *de novo*, and used to construct larger virtual combinatorial libraries. These compounds can then be screened *in silico* prior to going to the effort of synthesising and testing them.⁴¹ Alternatively, computational methods can also be used for *in silico* screens of data bases of commercially available compounds. A number of software packages are available that cater for these purposes, for example LUDI,⁴³ used for fragment build-up approach for the design of leads, or DOCK⁴⁴⁻⁴⁶ which uses distance matching for the placement of potential leads into receptor sites, primarily used for the screening of data-bases of compounds. In addition, aspects of these methods are also helpful for the design of derivatives once a lead has been identified, as part of the lead optimisation process.

The program LUDI⁴³ can be used for either data base searching or alternatively for a fragment build-up approach for *de novo* design of ligands (reviewed in Joseph-McCarthy⁴¹). This package uses a combination of statistical data from small-molecule crystal structures, or geometric rules or output from the program GRID⁴⁶ to identify potential interaction sites on the target receptor. Molecular fragments (taken from a library of hundreds) are placed into candidate binding sites so they can make favourable hydrogen bonding or hydrophobic interactions, whilst being connected with up to three other fragments (similarly placed into proximal sites) with simple linking groups (eg CH₂). Additional linkages may be made to larger optimised fragments to develop larger molecules. LUDI has a built-in scoring function that considers hydrogen bonding, ionic interactions, lipophilic contacts, and the number of rotatable bonds in the ligand. These components are based on experimental data from 45 known protein-ligand complexes. As LUDI predictions are based entirely on geometric considerations, it is very fast and can be used to predict protein-ligand complex structures. Hence LUDI can be used to identify novel pharmacophores.

However, it may be argued that *de novo* design of new compounds as potential leads is of limited value, particularly if the designed compounds are difficult to synthesise: a chemist may spend a lot of time synthesising a potential ligand that does not bind the target protein. Therefore, the preferred approach for the identification of leads by computational methods is to screen libraries of commercially available compounds. Also, a general limitation of *in silico* screening is that suggested leads often have poor solubility.

1.3.2 NMR methods in drug development

Nuclear Magnetic Resonance Spectroscopy (NMR) is a powerful tool in drug development. The method can be used for screening target molecules, but has the added advantage of being able to provide detailed structural information about identified binding interactions. As long as the chemical shifts have been assigned, the 2D [¹H,¹⁵N] Heteronuclear Single Quantum Coherence (HSQC) experiment⁴⁷ with uniformly ¹⁵N labelled protein provides a method for testing individual molecules, or screening large libraries of compounds for binding.⁴⁸ Changes in chemical shift for receptor-ligand mixtures relative to the free receptor indicate binding events. Residues that are involved in binding can be identified directly, and where the 3D structure for the receptor is available, chemical shift changes can be mapped to the structure of the receptor. In addition, the method can also be used to calculate equilibrium dissociation constants, (K_d). If the ligand binds in slow exchange on the NMR chemical shift time-scale, the 3D structure of the protein-ligand complex can also be determined using NMR methods.

The work in the laboratory of Fesik⁴⁸ led to the rapid identification of a nanomolar affinity ligand for FK506 binding protein, using aspects of the above approach. By screening libraries of compounds, they were able to identify two weakly binding molecules that bound at two proximal sites on the receptor. Using the 3D structure of this complex as a guide, suitable linkers were synthesised that joined the two molecules together providing the nanomolar ligand. This and subsequent work with development of strong inhibitors for Stromelysin⁴⁹ also illustrates the power of the general concept of identifying two or more weakly bound ligands for proximal sub-sites on a protein structure, and obtaining a large improvement in binding affinity by joining the ligands together.⁵⁰

1.4 2-Aminoquinoline as a Tec SH3 domain small-molecule ligand⁵¹

Development of small molecule ligands for protein targets has been a long-term interest and goal in our research group. Creation of high affinity ligands for a specific protein is not only a common approach used by the pharmaceutical industry for development of new medicines (as discussed in Section 1.3), but high affinity ligands may also be used as probes for elucidation of the functions of bio-molecules. The Tec family of non-receptor protein tyrosine kinases is one such family where the function of the bio-molecule remains unclear. Therefore, we have used the Tec SH3 domain, as a model system for structure based drug design. The 3D structure of the SH3 domain of the Tec IV enzyme in the mouse was solved

by NMR methods^{13,52} (Figure 1-1) and the binding surface of a proline-rich peptide ligand for this domain was characterised.¹³

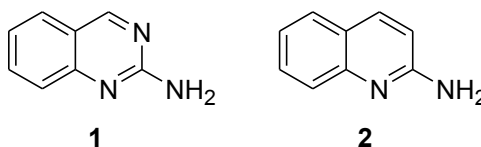


Figure 1-9: Structures of heterocyclic compounds 2-aminoquinazoline **1** and 2-aminoquinoline **2**.

Using the identified peptide ligand binding surface, *in silico* screening of small molecule fragments was performed with the LUDI⁴³ molecular modelling package. From these studies, it was predicted that the simple heterocycle 2-aminoquinazoline **1** (Figure 1-9) would bind to the Tec SH3 domain at conserved residues in the specificity pocket of the proline-rich peptide site. However, at this stage **1** was not immediately available for testing, as it could not be obtained from commercial sources. But, the structurally related compound, 2-aminoquinoline **2** (Figure 1-9) was readily available. Compound **2** was therefore tested for binding to the Tec SH3 domain using NMR chemical shift perturbation with [¹H,¹⁵N] Heteronuclear Single Quantum Coherence (HSQC) experiments, with uniformly ¹⁵N labelled protein, and this indicated that **2** bound the SH3 domain (Figure 1-10A). Mapping the changes in ¹H (H-N) chemical shift induced by **2** onto the SH3 domain structure indicated that the ligand bound at or near the location specified by the LUDI ligand design (Figure 1-10B). Amino acid residues whose ¹H (H-N) chemical shifts were altered by at least 0.1 ppm at or near saturation binding of **2** were used as monitors for the determination of equilibrium binding dissociation constants, K_d , and the K_d for **2** was calculated as 125 μ M (Figure 1-11, Table 1-2).

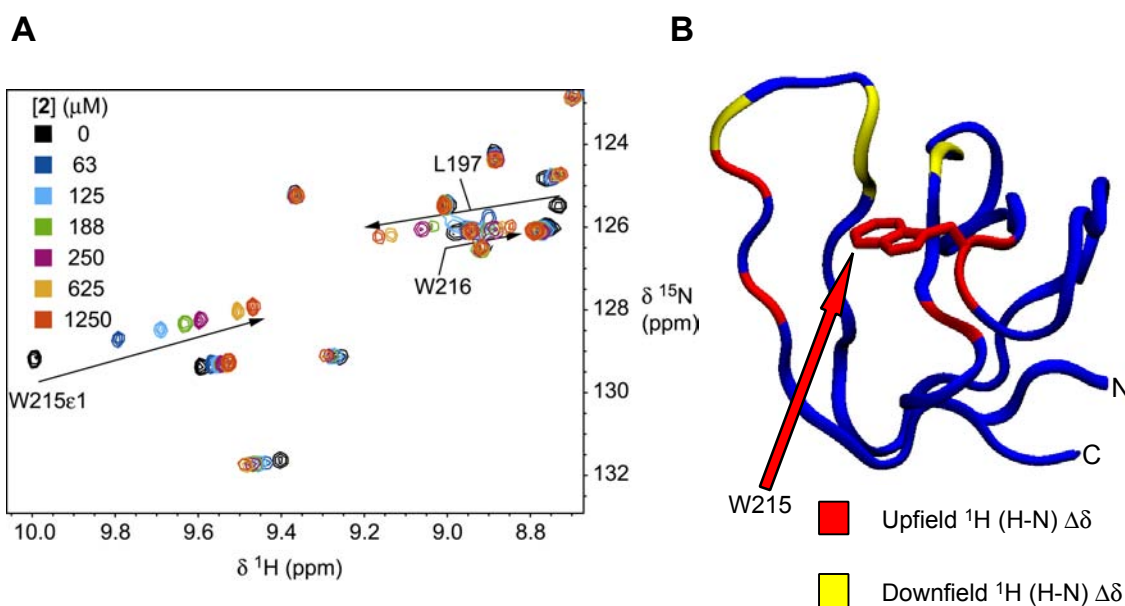


Figure 1-10: Binding of **2** to the Tec SH3 domain as studied by NMR spectroscopy. (A) A region of overlaid NMR [^1H , ^{15}N] HSQC spectra of ^{15}N -labelled Tec SH3 protein in the presence of increasing concentrations of **2**. (B) Chemical shift mapping of residues whose backbone or side-chain resonances, $\delta^1\text{H}$ (H-N) had changed by at 0.1 ppm at or near saturation binding of **2**.

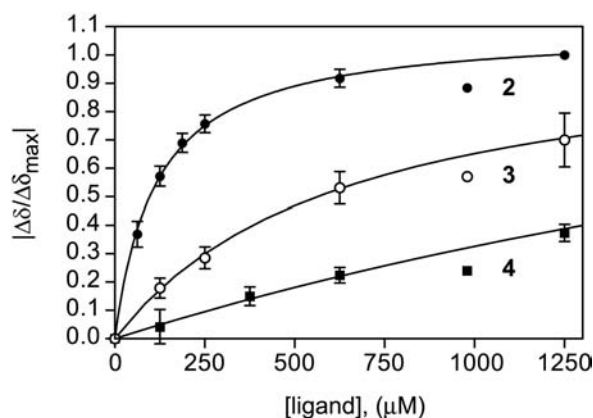


Figure 1-11: Equilibrium binding isotherms represented by the mean of normalised chemical shift changes for residues involved in binding of ligands **2**, **3** and **4**, as determined by the NMR chemical shift perturbation experiments.

A small series of commercially available compounds structurally related to **2** (Figure 1-12) were subsequently tested for binding to the Tec SH3 domain, again using the NMR chemical shift perturbation method, and a further two ligands were identified (Figure 1-11, Table 1-2). The positional isomer of **2**, 1-aminoisoquinoline **3** bound the SH3 domain with approximately five-fold reduced affinity ($K_d = 650 \mu\text{M}$) relative to **2**, however the single ring equivalent of **2**, 2-aminopyridine **4**, bound the SH3 domain very weakly ($K_d > 4000 \mu\text{M}$). Quinolin-2(1*H*)-one **5** in which the functionality at the 2-position differs to **2** was unable to bind to the SH3 domain.

Similarly, when the 2-amino functionality was removed as for quinoline **6**, or the ring nitrogen was removed as for 2-aminonaphthalene **7**, binding was also abolished.

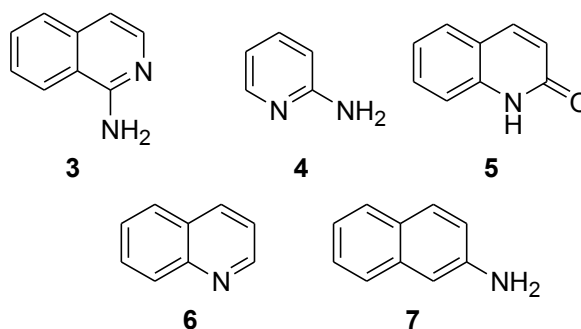


Figure 1-12: Structures of additional (commercially available) compounds tested for binding to the Tec SH3 domain.

Table 1-2: Binding studies of the first series of compounds tested for binding to the Tec SH3 domain using NMR spectroscopy

Compound	K_d (μM)*	$\text{p}K_a$	Compound	K_d (μM)*	$\text{p}K_a$
2	125 ± 24	7.34^{53}	5	no binding	-
3	650 ± 90	7.62^{54}	6	no binding	-
4	> 4000	6.86^{53}	7	no binding	-

* Quoted values are mean \pm standard deviation over residues where ^1H (H-N) chemical shifts were altered by at least 0.1 ppm at or near saturation binding of ligand.

The structure activity information provided by testing all of the above compounds (Figures 1-9 and 1-12), in conjunction with the NMR chemical shift perturbation experiments, were used to propose a model for the mechanism of the binding of **2** to the Tec SH3 domain. A key aspect that assisted in developing this model was the realisation that the ligands that bound the SH3 domain were likely to be substantially protonated on the pyridyl ring nitrogen atom under the experimental conditions, and hence positively charged ($\text{p}K_a$ s given in Table 1-2). In this model, the quinoline ring is involved in π - π stacking with the indole side-chain of the tryptophan 215 (W215) residue, and a salt bridge is formed between the positively charged ligand and the negatively charged aspartate 196 (D196) residue as illustrated in Figure 1-13. As the ligand binding of **2** (the highest affinity ligand identified at this stage) is in fast exchange on the NMR timescale, then there is not sufficient time for inter-molecular Nuclear Overhauser Effect (NOE) build-up and transfer between the ligand and the protein. Measurement of these NOEs forms the basis for determination of 3D structures of ligand/protein complexes. Thus, a 3D structure of the **2**/SH3 complex is not available to provide conformation of the proposed ligand binding model.

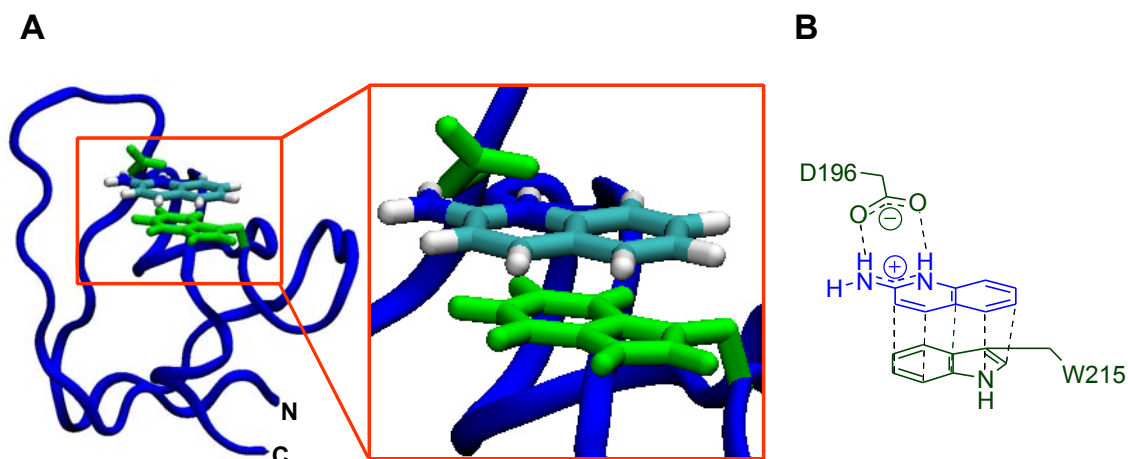


Figure 1-13: Proposed model for the binding of 2-aminoquinoline **2** to the Tec SH3 domain. (A) Model illustrated on the protein structure, the two key residues from the SH3 domain (W215 and D196) are illustrated in green, and **2** aqua. (B) Cartoon representation: W215 and D196 in green, **2** in blue.

In order to confirm overlap between the **2** and proline-rich peptide binding sites for the Tec SH3 domain, a Fluorescence Polarisation (FP) peptide competition assay was developed by a co-worker, Cvetan Stojkoski. A proline-rich peptide derived from a sequence previously used in binding studies with the Tec SH3 domain¹³ was obtained with fluorescein attached at the N-terminus via a β -alanine linkage (fluorescein- β A-RRPPPPPIPPE-CO₂H, here after referred to as **PRP-1**). Using FP, the binding of **PRP-1** to both the Tec SH3 protein, and Glutathione-S-Transferase-SH3 (GST-SH3) fusion protein was demonstrated, and the calculated equilibrium binding dissociation constants (K_d s = 174, and 167 for SH3 and GST-SH3 respectively) indicated that the affinity was similar in each case (see Section 2.3.1 Chapter 2). This indicates that the presence of the GST fusion partner has little influence on the binding of **PRP-1** to the SH3 domain. Therefore, preliminary FP experiments were performed using the GST-SH3 fusion protein. The ability of **2** to displace **PRP-1** from the SH3 domain was then demonstrated (Figure 1-14). The ligand concentration required to displace 50% of **PRP-1** (EC_{50}) from the GST-SH3 fusion protein by **2**, was determined by maintaining a constant concentration of **PRP-1** and GST-SH3 protein, and varying the concentration of **2**. The normalised Δ mP (proportion **PRP-1** bound) was then plotted against the concentration of **2** (Figure 1-14) and the EC_{50} was calculated following non-linear regression analysis, with the software Prism.⁵⁵ Ligand **2** was able to compete with **PRP-1** for binding to the Tec GST-SH3 protein with an EC_{50} of $160 \pm 35 \mu\text{M}$, providing confirmation of overlap between the **2** and **PRP-1** binding sites. To test the role of D196 in binding **2** to the SH3 domain, a series of SH3 mutants (D196A, D196E, D196N and D196T) were prepared

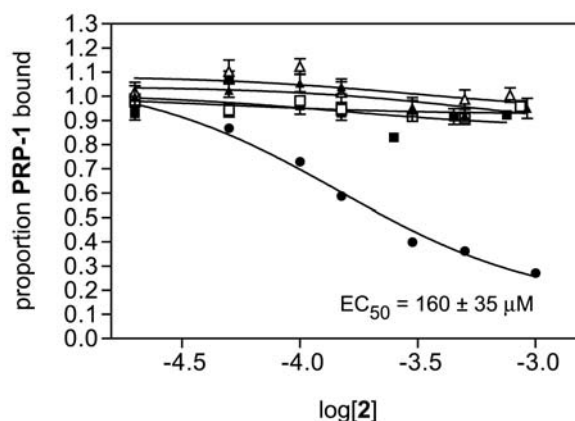


Figure 1-14: Fluorescence Polarization studies of Tec SH3 domain with fluorescently labelled proline-rich peptide [Fluorescein- β A-RRPPPPPIPPE-CO₂H (**PRP-1**)]. Binding isotherms for competition of **PRP-1** by **2** from wild-type and mutant Tec GST-SH3 proteins.

as GST-SH3 fusion proteins. These proteins bound **PRP-1** with reduced affinity (data not shown), however **2** was unable to displace **PRP-1** from any of these mutant proteins (Figure 1-14). These results provide evidence for the importance of D196 for the binding of **2** to the SH3 domain, and support for the proposed ligand binding model (Figure 1-13), in the absence of a 3D structure of the **2**/SH3 complex.

1.5 Aims and approach for PhD project

At the commencement of this work, there were several aims proposed for the project. Ultimately, the plan was to develop high affinity and highly specific small-molecule ligands for the Tec SH3 domain. To achieve this goal, the proposed work was divided into two minor and two major aims.

The first minor aim of the project was to continue to characterise the 2-aminoquinoline/Tec SH3 binding event, as a means of confirming and/or refining the proposed 2-aminoquinoline/SH3 ligand binding model presented in Section 1.4 (Figure 1-13). A few approaches would be used to achieve this aim. Firstly, simple 2-aminoquinoline derivatives and other heterocyclic compounds would be synthesised and tested for binding. Secondly, additional commercially available compounds structurally related to **2** would also be tested for binding to the Tec SH3 domain. The results from both of these approaches would provide new SAR information about the ligand binding event. In addition, it may lead to the identification of an alternative 'lead' compound with improved affinity. Thirdly, given that protonation of 2-aminoquinoline is likely to be important for binding to the SH3 domain, according to the ligand binding model (Figure 1-13), the effect of pH on the binding of **2**

would be investigated. The work associated with achieving these aims forms the basis of Chapter 2.

The first main aim of the project was to use the highest affinity 'lead' compound identified to develop higher affinity ligands. Two approaches, in conjunction with each other, would be used to achieve this aim. Firstly, the ligand binding model will form a basis for predicting appropriate functionality that could be incorporated onto the nucleus of the lead compound, that may make new interactions with the protein, and thereby enhance the affinity of the ligand. Secondly, methodology for the synthesis of a range of derivatives of the 'lead' compound will be explored. For example, synthesis of *N*-substituted 2-aminoquinolines, or ring-substituted 2-aminoquinolines would be investigated. The work associated with this aim forms the basis of Chapters 3 and 4.

The second main aim of the project was to identify a ligand suited to 3D structure determination of its complex when bound to the Tec SH3 domain using NMR methods. This would rely on a ligand that has an adequate improvement in affinity (or more specifically a ligand that is in slow exchange on the NMR time scale) being developed during the studies to be presented in Chapters 3 and 4. Slow exchange ligands are required for the measurement of Nuclear Overhauser Effects between two molecules, which forms the basis for structure calculations of a complex of two molecules. The derived structure will provide ultimate confirmation of the proposed ligand binding model, and assist in designing new 2-aminoquinoline derivatives (Section 1.4, Figure 1-13). Work associated with achieving this aim is presented in Chapter 4.

The second minor (and final) aim of this project was to investigate the specificity of 2-aminoquinoline (or other derivatives) with other SH3 domains. Given the high degree of conservation between the SH3 domains, it may be predicted that 2-aminoquinoline will bind to other SH3 domains. In any ligand development strategy targeted towards biological investigations, knowledge of the specificity of the ligand is of key importance. The work associated with satisfying this aim will be presented in Chapter 5.

Chapter 2

Additional Characterisation of the 2-Aminoquinoline/Tec SH3 Domain Binding Event

2.1 Introduction

As was presented in Chapter 1, it was discovered that 2-aminoquinoline **2** bound to the Tec SH3 domain with moderate affinity ($K_d = 125 \mu\text{M}$) and SAR, in conjunction with NMR chemical shift perturbation information, was used to develop a model for the mechanism of **2**/SH3 binding (Figure 1-13). In this model, there is π - π stacking between the quinoline ring and the indole side-chain of the tryptophan 215 (W215) residue, and there is a salt bridge between the aspartate 196 (D196) residue and the positively charged (and resonance stabilised) quinoline ring nitrogen atom (arising from protonation of the quinoline ring nitrogen atom under the experimental conditions). However, because the ligand binding is in fast exchange on the NMR timescale, it is not possible to determine the structure of the **2**/SH3 complex using NMR methods, and hence confirm this ligand binding model.

In this chapter, a number of approaches will be described that were used as a means to further investigate the mechanism of **2**/Tec SH3 domain binding. These include the synthesis of some simple 2-aminoquinoline derivatives, and testing of these and other commercially available compounds for SH3 domain binding. In addition, some other derivatives were donated or synthesised by colleagues, and these were also tested for binding. Given that protonation of **2** is likely to play a key role in the binding of **2** to the Tec SH3 domain, the effect of pH on the binding of **2** was also investigated. All the new SAR information obtained in these studies will then be discussed, and the **2**/SH3 domain binding model is refined.

Also as presented in Chapter 1, all of the preliminary ligand binding experiments used the NMR chemical shift perturbation method with uniformly ^{15}N labelled SH3 protein. However, later a Fluorescence Polarisation (FP) peptide displacement assay was also described, that was used to confirm overlap of the **2** and proline-rich peptide ligand binding sites. As part of the investigations presented in this chapter, some significant features of the FP method were also investigated, and important comparisons between the FP and NMR methods were made. A discussion of this is also included in this chapter.

2.2 Synthesis of some simple 2-aminoquinoline derivatives

In this section, the synthesis of three simple 2-aminoquinoline derivatives is presented. Two of these compounds, the *N*-substituted derivatives (*N*-methyl)quinolin-2-ylamine **8** and *N*-(quinolin-2-yl)acetamide **9** (Figure 2-1) were selected for synthesis as it was anticipated that they would give information about the importance of the amino group of 2-aminoquinoline for binding to the SH3 domain. Given that a salt bridge involving this amino group is proposed to be one of the key interactions in the ligand binding event, the binding results from these *N*-substituted compounds were anticipated to provide very useful information. Specifically, it was of interest to investigate the effect of placement of a small alkyl group on the amino functionality in the case of **8**, however in the case of **9**, the influence of functionality that substantially alters the basicity of the amino group was sought.

The other derivative that was selected for synthesis was 2-amino-5,6,7,8-tetrahydroquinoline **10** (Figure 2-1). It was anticipated that this compound would provide information about the optimal chemical composition of the second ring in a bicyclic system such as 2-aminoquinoline **2**. Given that 2-aminopyridine **4** which lacks the second ring of **2** binds so weakly relative to **2** ($K_d > 4000 \mu\text{M}$ and $125 \mu\text{M}$ for **4** and **2** respectively, Section 1.4) it was of interest to investigate whether aromaticity of this second ring was necessary for optimal affinity.

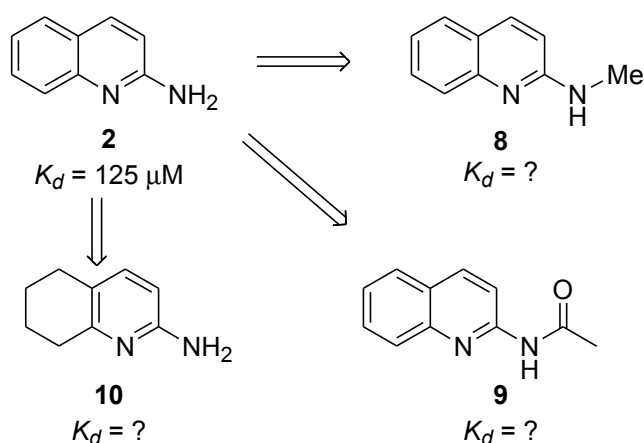
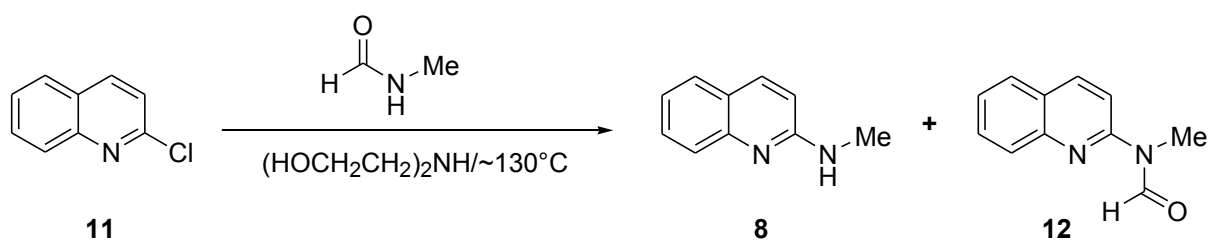


Figure 2-1: Three simple 2-aminoquinoline derivatives (sought for obtaining new SAR information about the 2-aminoquinoline/SH3 domain binding event), the synthesis of which is presented in this chapter.

2.2.1 Synthesis of (*N*-methyl)quinolin-2-ylamine

(*N*-Methyl)quinolin-2-ylamine **8** was prepared by treatment of 2-chloroquinoline **11** with *N*-methylformamide and diethanolamine at ca. 130°C for 12 hours, according to a literature method (Scheme 2-1).⁵⁶ Following workup and purification twice by silica gel chromatography, **8** was isolated in very low yield (1%), in conjunction with a by-product, the *N*-methyl-*N*-formyl derivative **12** (Scheme 2-1) in 3% yield. The main reason for the poor yield is likely to be due to substantial losses during the reaction workup: it is possible that some material was lost to the aqueous layer due to insufficient water usage during the workup, given the high water solubility of both *N*-methylformamide and diethanolamine. In addition, substantial loss of product may have occurred during the first chromatographic procedure, because the eluant was not sufficiently polar to efficiently elute all the material off the column. Furthermore, given that the *N*-methyl-*N*-formyl by-product (likely to be an intermediate in the formation of **8**) was also isolated suggests that the reaction had not proceeded to completion, and thus the reaction conditions were not optimal. Despite the poor yield, enough of **8** was isolated to perform the ligand binding experiments.



Scheme 2-1: Synthesis of (*N*-methyl)quinolin-2-ylamine **8** according to the method of Cho.⁵⁶

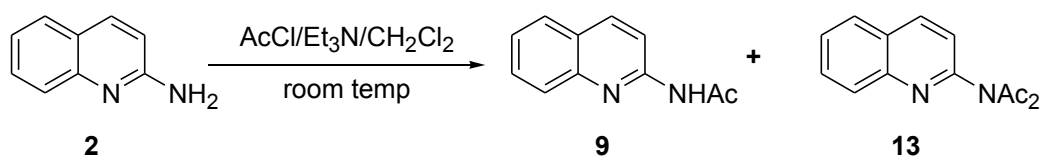
Features of the ¹H NMR spectrum of **8** that provided evidence for its structure included a large upfield shift of the signal for H3 in 2-chloroquinoline **11** from δ 7.38 ppm to 6.64 ppm in **8**, consistent with substitution of the chloride for a group with a markedly greater resonance donating effect. A broad singlet at δ 4.77 ppm was also observed for the amino NH proton, in addition to the appearance of a doublet with *J* = 4.8 Hz at δ 3.09 ppm for the methyl protons coupling to the NH proton. In addition, the melting point of **8** was consistent with that given in the literature.

The evidence for the formation of the by-product **12** in the ¹H NMR spectrum included a smaller upfield change in chemical shift (relative to that described for **8** above) for the H3 proton of 2-chloroquinoline from δ 7.38 ppm to 7.25 ppm in **12**. In addition, a singlet was observed at δ 3.49 for the methyl group, and a singlet at δ 9.52 ppm was suggestive of a formyl proton. There was also a signal at δ 162.5 ppm in the ¹³C NMR spectrum, and an IR

band at 1679 cm^{-1} both indicative of a CO group. The identity of **12** was also confirmed by mass spectrometry.

2.2.2 Synthesis of *N*-(quinolin-2-yl)acetamide

N-(Quinolin-2-yl)acetamide **9** was synthesised by treatment of 2-aminoquinoline **2** with two equivalents of acetyl chloride in the presence of triethylamine in dichloromethane at room temperature as illustrated in Scheme 2-2. Following workup, ^1H NMR spectroscopy suggested that a mixture of two products had formed. The crude product was therefore purified by chromatography on silica gel and the desired product **9** was isolated in 46% yield, accompanied by the diacetylated derivative **13** in 33% yield. Although formation of the by-product **13** can be rationalised given that two equivalents of acetyl chloride were used for the reaction, **13** was not expected to form as a mono-acetylated product such as **9**, would not normally be expected to undergo a second acetylation.



Scheme 2-2: Synthesis of *N*-(quinolin-2-yl)acetamide **9**.

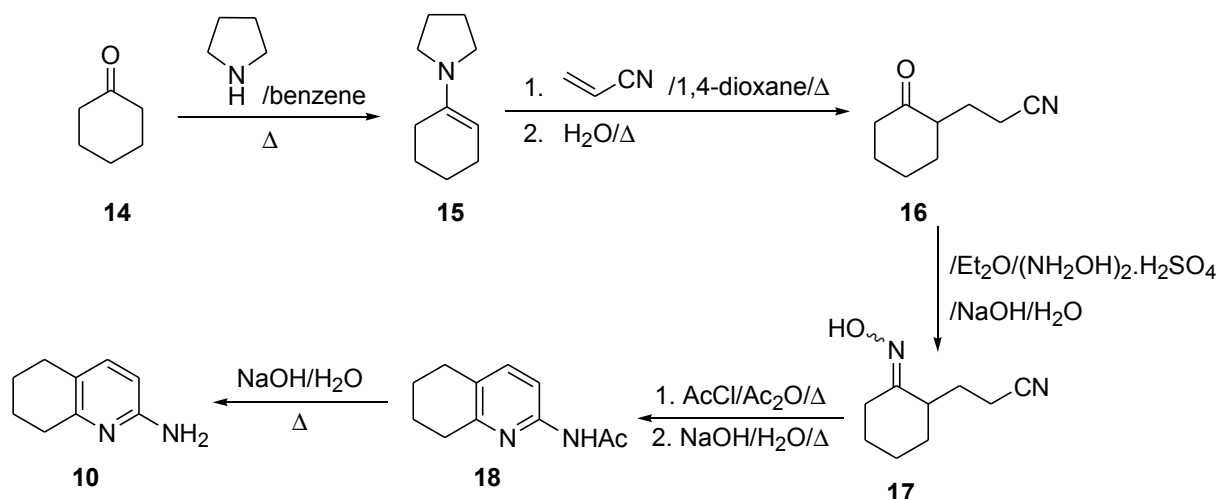
Evidence for the formation of **9** included a large downfield change in chemical shift in the ^1H NMR spectrum for the H3 proton on the quinoline ring from δ 6.72 ppm in **2** to a broadened doublet at 8.42 ppm in **9**. The broadening of this signal is most likely a consequence of intermediate exchange on the NMR timescale between rotamers around the amide, and/or the HN–C(quinoline ring) bonds. The assignment of this signal to H3 was confirmed, given that assignment of the signal to H4 could be eliminated based on the observation of a through space correlation between the H4 and H5 protons of the quinoline ring, using a [$^1\text{H}, ^1\text{H}$] ROESY spectrum. In addition, a signal was observed at δ 2.20 for the methyl group of the acetyl motif, and a signal was observed at 1674 cm^{-1} in the IR spectrum indicative of a carbonyl group. The melting point of **9** was also consistent with that presented in the literature.

Features of the ^1H NMR spectrum that provided evidence for the formation of **13** included a 6-proton singlet at δ 2.38 ppm suggestive of the presence of two methyl groups ($2 \times \text{CH}_3\text{CO}$), and the loss of the broad NH signal observed in **9**. In addition, there was an upfield change in chemical shift of the H3 proton from δ 8.42 ppm in **9** to 7.33 ppm in **13** and the broadening of

the signal was also no longer observed. A signal at δ 172.6 ppm in the ^{13}C NMR spectrum was suggestive of a large quaternary signal relative to other quaternary signals, suggestive of the presence of two carbonyl groups. In addition, bands at 1730 and 1698 cm^{-1} in the IR spectrum were indicative of asymmetric and symmetric stretches respectively of the carbonyl groups of the diacetyl motif. The identity of **13** was confirmed by both mass spectrometry and elemental analysis.

2.2.3 Synthesis of 2-amino-5,6,7,8-tetrahydroquinoline

2-Amino-5,6,7,8-tetrahydroquinoline **10** is a known compound, with its synthesis reported in four steps starting from cyclohexanone **14** as illustrated in Scheme 2-3.^{57,58} In this method, cyclohexanone **14** is treated with pyrrolidine to form enamine **15**, which is subsequently treated with acrylonitrile to form a Michael addition product that is hydrolysed in the same 'pot' to form the cyano-cyclohexanone derivative **16**.⁵⁷ Treatment of **16** with hydroxylamine provides the 3-[(2-hydroxyimino)cyclohexyl]propionitrile derivative **17**, which on treatment with acetyl chloride and acetic anhydride undergoes an *O*-acetylation, followed by a rearrangement and a cyclisation process, and finally an *N*-acetylation to afford *N*-(5,6,7,8-tetrahydroquinolin-2-yl)acetamide **18**.⁵⁸ By addition of aqueous sodium hydroxide to the same 'pot' followed by further heating at reflux, 2-amino-5,6,7,8-tetrahydroquinoline **10** is then formed.



Scheme 2-3: Method for synthesis 2-amino-5,6,7,8-tetrahydroquinoline **10** according to the method of Vijn.⁵⁸

The above approach was therefore tested here. Enamine **15** was synthesised by treatment of **14** with two equivalents of pyrrolidine and heating at reflux with a Dean Stark apparatus attached for 5 hours as illustrated in Scheme 2-3. According to the literature procedure for preparation of **15**, the crude product can be used in the subsequent alkylation step without purification. However, when the method was tried here, the mass of the crude product

suggested that a substantial excess of pyrrolidine and/or benzene remained in the sample. Thus, the product was distilled under reduced pressure, to afford pure **15** in 77% yield. Enamines are not particularly stable compounds (as they are readily hydrolysed back to carbonyl compounds), thus, it is generally preferable to use them in alkylation steps promptly. However, they may be stored for short periods of time under an inert atmosphere in a refrigerator.⁵⁷ With this in mind, little spectroscopic data for **15** was obtained. Comparison of the boiling point of **15** obtained here with that in the literature was not informative as the pressures used for distillation were markedly different.

The purified enamine **15** was then converted to the cyclohexanone derivative **16** by treatment with acrylonitrile in 1,4-dioxane with heating at reflux overnight as illustrated in Scheme 2-3. Water was then added to the reaction mixture and heating at reflux was continued for a further 1.5 hours. Following workup and purification by distillation under reduced pressure, **16** was isolated in 64% yield. Again, comparison of the boiling point of **16** obtained here with that in the literature was not informative, due to differences in the pressures of the vacuums used. The ¹H NMR spectrum of **16** indicated that the product was highly pure, however, no assignments of the signals were made, as every signal was a complex multiplet. However, the IR spectrum provided good evidence for the existence of carbonyl and cyano functionality in the molecule, as bands at 1708 (CO) and 2245 cm⁻¹ (C≡N) were observed.

Cyclohexanone derivative **16** was converted to the hydroxyimino-derivative **17** in 53% yield by treatment of **16** with a slight excess of hydroxylamine (as the hydrogen sulfate salt) in the presence of sodium hydroxide in a mixture of water and ether as illustrated in Scheme 2-3. Again the ¹H NMR spectrum of **17** was too difficult to assign, however the IR spectrum, in which bands at 2241 cm⁻¹ (C≡N) and 1642 cm⁻¹ (C=N-O) were observed, provided some assistance with characterising **17**. However, consistent with the literature procedure, crude **17** was used in the subsequent step without purification. Hence **17** was treated with an excess of both acetic anhydride and acetyl chloride and heated at reflux for 4.5 hours, as illustrated in Scheme 2-3. After cooling, aqueous sodium hydroxide was added to the mixture and heating at reflux was continued for a further 3 hours. Following workup a black tar was isolated and ¹H NMR suggested that the main product present in the mixture was the *N*-acetylated-2-amino-5,6,7,8-tetrahydroquinoline derivative **18**, in contrast to the literature where the free amine **10** was the major product following the same reaction conditions. Thus, half of the material was purified by column chromatography on silica gel to afford purified **18** in 8% yield. The main evidence in the ¹H NMR spectrum for the structure of **18** was the presence of two doublets at δ 7.88 and 7.34 ppm with *J* = 8.3 Hz. Although these chemical

shifts are more upfield relative to the H3 and H4 protons in the *N*-acetyl-2-aminoquinoline derivative **9** described above, the signal at δ 7.88 (tentatively assigned to H3) is too far downfield to be consistent with the chemical shift expected in a 2-aminoquinoline. Furthermore, the signal at δ 7.88 was broadened, in a similar fashion to that observed for the H3 proton of **9** described above. In addition, a signal was observed at δ 2.14 ppm suggestive of a methyl group. The chemical shifts were also in good agreement with those presented in the literature for **18** and the identity of the material was confirmed by mass spectrometry.

The purified sample of **18** was then treated overnight with aqueous sodium hydroxide at reflux temperature, and following workup, pure **10** was isolated in 49% yield. Evidence for the formation of this product included loss of the singlet at δ 2.14 ppm observed in **18** for the methyl group of the acetyl motif, and an upfield change in chemical shift for the H3 proton of the quinoline ring from δ = 7.88 ppm in **18**, to 6.30 ppm in **10**. In addition, the broadening of this signal was no longer observed. Furthermore, these chemical shifts, and the melting point were also in good agreement with those presented in the literature.

2.3 Additional investigation into the Fluorescence Polarisation (FP) method for testing of compounds for SH3 domain binding

In Chapter 1 (Section 1.4) the Fluorescence Polarisation (FP) technique was introduced. There were several reasons for the development of this assay as part of the current work. Firstly, during the early stages of characterising the 2-aminoquinoline **2**/SH3 domain binding event, the method served the key role of confirming that **2** bound the SH3 domain at part of the proline-rich peptide binding site. Secondly, the same method was subsequently used to test the role of aspartate 196 (D196) for **2**/SH3 binding, using a series of D196 mutant proteins. Another motive for developing the method in our laboratory was to provide us with another tool for the testing of compounds for binding to the SH3 domain. Use of the FP method for both peptide binding, and ligand competition assays has been well documented.⁵⁹⁻⁶¹ When compared to the NMR chemical shift perturbation method, the FP method has advantages such as improved efficiency, and lower cost, that added to the appeal for developing the method for our use.

In this section, the results from some important experiments that were performed as a means of learning more about the FP method, with particular relevance to applying the method to the current study, are presented.

2.3.1 SH3 vs GST-SH3 proteins in the FP assay: A comparison of results

In the early stages of developing the FP assay as a new tool in the current ligand development studies, one of the key aspects that needed to be addressed was which SH3 protein constructs could be used. More specifically, the question was posed: was the method suited to the GST-SH3 fusion protein, or was it necessary to use the cleaved, purified SH3 domain? Use of the GST-SH3 domain would be preferable from the point of view that it is quicker to prepare the GST-SH3 fusion protein: the need to enzymatically cleave and subsequently purify the protein is removed, and hence the yields of protein are higher.

For the following discussion, an overview of the theory behind FP is first needed. In FP, the degree of binding of a 'tracer' molecule (a molecule that is covalently linked to a fluorophore) to another molecule can be detected, following excitation of the tracer with plane polarised light. The degree of polarisation of light with wavelength corresponding to the wavelength of emission of the fluorophore then serves as a monitor for the binding of the two molecules. When binding occurs, the molecular mass of the 'complex' is greater than that of the tracer alone. Thus, the relative rate of rotation of the fluorophore is decreased, and the amount of de-polarisation of the emitted light is also reduced. Hence, the polarisation P ,⁶⁰ is increased according to the definition of P as:

$$P = (Int_{\parallel} - Int_{\perp}) / (Int_{\parallel} + Int_{\perp}),$$

where Int_{\parallel} = intensity of emission in the plane parallel to the plane of excitation, and Int_{\perp} = intensity of emission in the plane perpendicular to the plane of excitation.

In the current study, the tracer molecule is a fluorescently labelled proline-rich peptide (fluorescein- β A-RRPPPIPPE-CO₂H, hereafter referred to as **PRP-1**). In order to investigate the effect of the GST fusion partner, **PRP-1** binding and **2/PRP-1** competition assays were performed with both proteins. As can be seen in Figure 2-2A and Table 2-1, there is not a significant difference in the K_d values obtained for the binding of either the GST-SH3 or SH3 proteins to **PRP-1** (K_d s = 167 and 174 μ M for GST-SH3 and SH3 respectively). This suggests that the presence of the GST fusion partner has no influence on the binding of **PRP-1** to the SH3 domain. However, it is clearly evident in Figure 2-2A, that the changes in polarisation (ΔmP values) that are obtained at the same concentration of SH3 construct are significantly higher in the case of the GST-SH3 construct. Given the definition of P as described above, and the considerably higher molecular mass of the GST-SH3 protein relative to the cleaved SH3 domain (~ 32 vs 8 kDa), this observation is consistent with the theory.

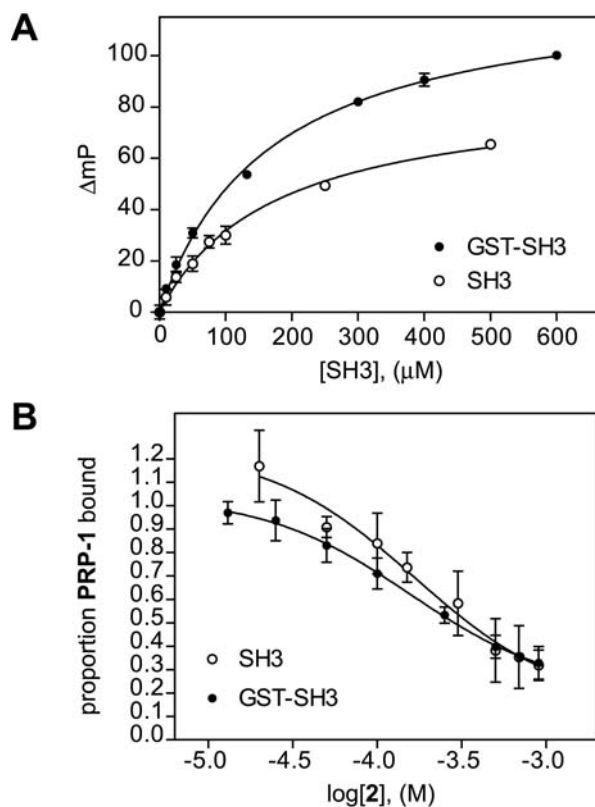


Figure 2-2: Investigation into influence of GST fusion partner on Fluorescence Polarisation (FP) studies with Tec SH3 domain with fluorescently labelled proline-rich peptide **PRP-1**. (A) Equilibrium binding isotherms of SH3 and GST-SH3 fusion proteins to **PRP-1**. (B) Isotherm for competition of **PRP-1** by **2** from the Tec SH3 and GST-SH3 fusion proteins.

Table 2-1: Comparison of binding constants derived from Fluorescence Polarisation (FP) experiments using either GST-SH3 or SH3 protein constructs.

Protein Construct Used	Equilibrium Binding of PRP-1: K_d (mM) [†]	Ligand 2 Peptide Competition EC_{50} (mM) [†]
GST-SH3	167 ± 29	160 ± 35
SH3	174 ± 23	162 ± 22

[†] Quoted values are mean \pm standard deviation over three replicate experiments.

This increased ΔmP at lower protein concentration is of considerable benefit when considering the difference in the signal to noise between the two protein constructs: when the larger protein construct is used, the signal to noise is greatly increased at lower protein concentrations. Whilst this is of little consequence when applied to peptide binding experiments alone (as evidenced by the existence of very small error bars in Figure 2-2A), it is clearly of consequence on inspection of the errors associated with the replicates in the **2/PRP-1** competition assays, where the GST-SH3 and SH3 constructs were compared (Figure 2-2B). In each case, the concentration of protein used for the competition assays was

~ 120 μM . Using the equilibrium binding isotherms obtained for GST-SH3 vs SH3 in Figure 2-2A, it can be seen that the ΔmP values are about 60 and 30 mP units for the GST-SH3 and SH3 proteins respectively. Thus, in the case of the SH3 protein, because the overall signal is approximately halved compared to the GST-SH3 protein, the variation between replicates using standardised data results in much larger error bars. Comparison of the two isotherms indicates that there is indeed some difference between them, particularly at the lower ligand concentrations. However closer to the middle and end-points, little difference between the isotherms is evident. Given the size of the error bars at some of the lower ligand concentrations, the differences in the binding isotherms could be considered insignificant. Furthermore, the EC_{50} value should in theory reflect the ligand concentration required to displace 50% of the binding of **PRP-1** to the SH3 domain (ie. give proportion **PRP-1** bound = 0.5), and given that at this region of the two isotherms there is little difference between them, the inconsistency between earlier data points on the isotherms does not significantly impact on the calculated EC_{50} values (Table 2-1) between the two proteins. Despite this, it would be preferable if the size of the error bars, and thus the uncertainty associated with the calculated EC_{50} values could be eliminated.

Hence, based on the comparisons of both the K_d s and EC_{50} s derived from either the GST-SH3 and SH3 proteins, it may be concluded that it is valid to use the GST-SH3 fusion protein for FP experiments. Furthermore, given the improved signal to noise obtained with the GST-SH3 construct, the use of this protein is actually of considerable advantage. Since it is also easier to prepare the GST-SH3 protein as mentioned above, with the exception of the experiments presented in Section 2.4.2 (investigating the effect of pH on the binding of **2** to the SH3 domain), all future FP experiments were performed with the GST-SH3 protein construct.

2.3.2 Use of DMSO with the FP method

Another feature of the FP method that was also selected for investigation was the use of DMSO in the assay. When performing ligand binding experiments with small molecule compounds, it is often necessary to use a solvent such as DMSO, to assist dissolving a compound under aqueous conditions. This approach, with 10% DMSO in the aqueous buffer has been used for all the compounds tested by the NMR chemical shift perturbation method so far presented. During the early stages of development of the FP assay in our laboratory, it was assumed that the FP method would also be suited to the use of 10% DMSO in the buffer. However, when some compounds were tested with 10% DMSO in the buffer, it was noticed that the ΔmP values for the GST-SH3/**PRP-1** samples in the absence of any compounds (ie the control reading) were markedly lower than were previously observed at

the same protein concentration, in the absence of DMSO. Thus, based on the ΔmP values that were obtained in the presence of compounds, it was difficult to conclude whether or not the compound did indeed bind the protein. For example, a compound was tested by FP with 10% DMSO, and the data suggested that some binding was occurring, as small ΔmP values were observed (data not shown). When the same compound was tested using the NMR chemical perturbation method, no binding of the compound was observed (data not shown).

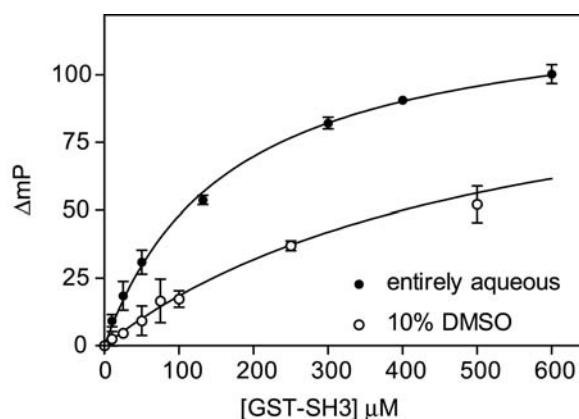


Figure 2-3: Investigation into influence of DMSO on the binding of **PRP-1** to the SH3 domain. Comparison of equilibrium binding isotherms obtained for binding of Tec GST-SH3 protein to **PRP-1** in a 10% DMSO/phosphate buffer system with that obtained under identical conditions but with the absence of DMSO. The experiment involving 10% DMSO was performed by Michaela Nicol.

Table 2-2: Investigation into influence of DMSO on binding of **PRP-1** to the Tec GST-SH3 fusion protein

Conditions Used	K_d (mM) [†]
Entirely aqueous	167 ± 29
10% DMSO*	540 ± 115

[†] Quoted values are mean \pm standard deviation over three replicate experiments. * This experiment was performed by Michaela Nicol.

Therefore, it was decided that an investigation into the influence of 10% DMSO in the aqueous buffer on the binding of **PRP-1** to the SH3 domain was warranted. Thus, the equilibrium binding of **PRP-1** to the Tec GST-SH3 protein was measured in the presence of DMSO using FP as illustrated in Figure 2-3 above. This experiment was performed by Michaela Nicol. On comparison of the binding isotherms obtained in the presence and absence of DMSO (Figure 2-3), it is clearly evident that **PRP-1** binds the SH3 domain considerably weaker in the presence of DMSO, and this is reflected in the K_d value (540 μM): an approximately three fold reduction in affinity (Table 2-2). Specifically, using a 10% DMSO system, a concentration of GST-SH3 fusion protein of $\sim 500 \mu\text{M}$ would be required to obtain

the same ΔmP values that could otherwise be obtained at [GST-SH3] of $\sim 100 \mu\text{M}$. The consequence of this is that, again, the signal to noise is significantly reduced. This explains how a 'false-positive' may have been obtained as described above for the early investigations. In order to reach the preferable level of signal to noise for ligand competition assays, a considerably higher concentration of protein would be required. Hence, fewer experiments could be performed using a 10% DMSO/buffer system, with the same amount of protein that would otherwise be used for experiments without DMSO in the buffer. Furthermore, the increased concentration of SH3 domain would also lead to a loss of sensitivity in the experiment, as higher concentrations of competing ligand would be required to observe displacement of **PRP-1**, given that an excess of the SH3 domain is always used.

Thus, as a result of this investigation, it was concluded a 10% DMSO/buffer system was not suited to performing **PRP-1**/small molecule ligand competition assays, and that compounds that were not sufficiently soluble in buffer alone could not be tested by the FP method. They would instead need to be tested by the NMR chemical shift perturbation method that is compatible with 10% DMSO (this matter will be further addressed in Section 2.3.3.2 below). The minimum level of solubility of a ligand required to obtain a sufficiently well defined competition binding isotherm using the FP method was $\sim 1.5 \text{ mM}$. It should also be noted that heating was frequently required to dissolve small molecule ligands in buffer alone.

Given that the binding pocket on the SH3 domains for the proline-rich peptide ligands is largely hydrophobic, it is possible that significant solvation between this pocket and the methyl groups of the DMSO molecules occurs. This could explain the reduced affinity of **PRP-1** for the SH3 domain in the presence of DMSO.

2.3.3 Comparison between FP and NMR methods for testing of compounds for SH3 binding

2.3.3.1 Advantages and disadvantages of the two methods

In comparison to the NMR chemical shift perturbation method that has also been described in this thesis, as a method for testing of compounds for binding to the Tec SH3 domain, the FP method has several advantages. Firstly, it was demonstrated above that use of the GST-SH3 fusion protein over the free SH3 domain is preferable for FP. This is quite advantageous, as fewer steps are required to prepare the protein samples for ligand binding assays.

Secondly, the FP method is considerably higher throughput for the determination of binding constants for ligands, whilst the NMR method is comparatively quite slow. Using NMR, to measure several spectra, in addition to manipulation of the sample (to add ligand) at each step, for just one compound, may take up to 10 hours. Then another two or three hours are typically required to process and analyse NMR data to extract and analyse chemical shift changes. Using the FP, the most time consuming component of the experiment is to prepare the 96 well plates with serially diluted compounds, protein, tracer etc. Once the plate is ready, the measurements only require a few minutes to be recorded. The data analysis is also much simplified compared to the NMR method. Typically two or three compounds can be tested and analysed in one day using FP.

On the other hand, there are some useful advantages with the NMR chemical shift perturbation method. Given that [$^1\text{H},^{15}\text{N}$] HSQC spectra are typically used for testing compounds, provided that the HSQC spectrum has been assigned, the residues involved in binding of the ligand are easily identified, and when the structure of the protein has also been solved (or if a homology model is available), the chemical shift changes can be mapped to the protein fold (as in Figure 1-13, Chapter 1). In addition, with particular application to the SH3 domains, FP is not compatible with a 10% DMSO/buffer system for performing small molecule/**PRP-1** displacement assays (refer Section 2.3.2), whereas the NMR method appears to be unaffected by DMSO in the buffer (as will be discussed further in the next section). This is advantageous in cases where ligands are insoluble in buffer alone.

2.3.3.2 Comparison of binding constants derived from FP and NMR methods

Another aspect of the FP and NMR methods that warrants discussion is comparison of the binding constants that are derived from each method. The NMR chemical shift perturbation method leads to the calculation of the equilibrium binding dissociation constant or K_d (see Appendix 1 for derivation). On the other hand, the binding constant obtained from the small molecule/peptide competition assay using FP, is called the EC_{50} . Theoretically, this refers to the concentration of ligand L, required to displace 50% of another molecule B (at constant concentration) that competes for binding to the target, eg a protein P. It is more difficult to describe the EC_{50} in terms of a series of equations as can be done for the K_d , because in this situation, three molecules are involved. Importantly, EC_{50} values should not be directly compared with a K_d . That is, an EC_{50} value for a ligand that was determined using a ligand competition assay will not necessarily be equal to the K_d determined for the same ligand using an alternative assay. The EC_{50} should be viewed only as an estimate of the K_d value. With this in mind, some caution needs to be used when comparing the binding constants

obtained between the FP and NMR methods, in particular for binding constants that might be generated by both methods for one particular ligand, as for **2** so far in this thesis. However, it seems reasonable to assume that the order of magnitude of the binding constants derived by either method should be consistent.

Despite the fact that EC_{50} and K_d should not be assumed to be equal, it is also important to note that in the current study, there are substantial differences between the experimental conditions in each method that may also influence the binding constants generated, for example pH, salt concentration, and the presence or absence of DMSO in the buffer. In NMR experiments, it is preferable to have the pH of the sample slightly more acidic than physiological pH of 7.3. This slows down the amide proton exchange rate, enhancing the signal to noise. Thus, all the NMR chemical shift perturbation experiments performed as part of this work were recorded at pH \sim 6.7. In addition, in order to avoid heating of the sample during NMR experiments, it is preferable to have a reduced concentration of sodium chloride in the buffer. For this reason, the NMR experiments here were performed in buffer alone without sodium chloride. It was also mentioned above that 10% DMSO is used to enhance water solubility of the ligands. In contrast, the conditions used in the FP assay much closer resemble physiological conditions: ie pH \sim 7.3, [sodium chloride] = 150 mM, and no DMSO. Despite these considerations, comparison of the EC_{50} value obtained for **2** ($160 \pm 36 \mu\text{M}$) using the FP method, with the K_d for **2** ($125 \pm 24 \mu\text{M}$) obtained using the NMR method, indicates that the binding constants derived from each method are similar. Furthermore, given this similarity, it may also be concluded that the presence of the DMSO in the buffer for the NMR derived K_d does not influence the binding of this ligand to the SH3 domain. This is in contrast to the binding of the proline-rich peptide **PRP-1** using FP as discussed in the previous section.

2.4 Binding studies of another set of compounds with the Tec SH3 domain: obtaining new SAR information

In this section, the binding of several compounds with structural similarities to 2-aminoquinoline **2** is presented. This includes the three compounds **8**, **9** and **10**, the synthesis of which were described in Section 2.2 (above), and the by-products **12** and **13** obtained in the synthesis of **8** and **9** respectively (Schemes 2-1 and 2-2). In addition three commercially available compounds (**19-21**) and three compounds that were synthesised by co-workers (**1**, **22** and **23**) as illustrated in Figure 2-4 were also tested. The testing of compound **1** was of particular interest given that this was the first compound predicted to bind to the Tec SH3

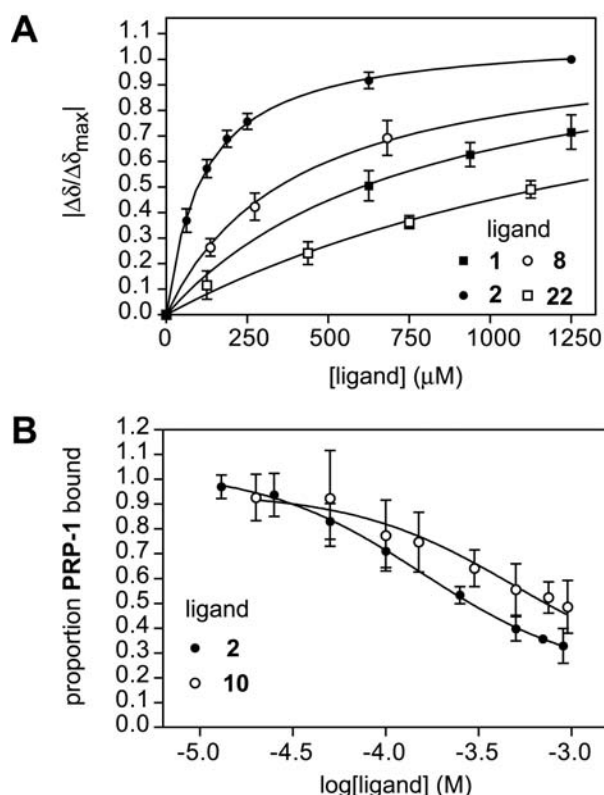


Figure 2-5: Ligand binding studies with the Tec SH3 domain, second series. (A) Overlays of binding isotherms (obtained from independent experiments) represented by normalised, averaged chemical shift changes for residues involved in binding of ligands **1**, **2**, **8** and **22**, as determined with NMR chemical shift perturbation experiments. (B) Overlays of competition binding isotherms (obtained from independent experiments) for competition of fluorescent proline-rich peptide **PRP-1** by **2**, and **10**, from Tec GST-SH3 protein using Fluorescence Polarisation Assay.

Table 2-3: Ligand binding studies of several compounds tested for binding to the Tec SH3 domain

Compound	K_d (mM) [†]	EC_{50} (mM) [*]	pK_a	Compound	K_d (mM) [†]	EC_{50} (mM) [*]	pK_a
2	125 ± 24	160 ± 36	7.34^{53}	13	No binding	-	-
1	800 ± 170	-	4.82^{62}	12	No binding	-	-
19	No binding	-	3.54^{63}	22	>1500	-	-
20	No binding	-	4.32^{64}	23	>3000	-	-
8	380 ± 40	-	-	10	-	480 ± 112	-
9	No binding	-	-	21	-	No competition	-

[†] Quoted values are mean \pm standard deviation over residues where ^1H (H-N) chemical shift changes of protein exceeded 0.1 ppm at or near saturation binding of ligand. ^{*} Quoted values are mean \pm standard deviation over 3 replicate experiments.

As determined with the FP peptide competition assay, 2-amino-5,6,7,8-tetrahydroquinoline **10** competed for binding with the proline-rich peptide **PRP-1** with approximately two-three fold reduced affinity relative to **2** (EC_{50} s 480 and 160 μM for **10** and **2** respectively) (Figure 2-

5B, Table 2-3). 2-Amino-8-hydroxyquinoline **21** was unable to compete for binding with **PRP-1** (Table 2-3).

2.4.2 Investigation into influence of pH on binding of 2-aminoquinoline to the Tec SH3 domain

One final approach was used to complete the characterisation of the mechanism of the binding of **2** to the Tec SH3 domain. As has now been well established, a clear role for D196 in the binding of **2** to the SH3 domain has been identified. Furthermore, it has also been demonstrated that ligands that are significantly protonated under the experimental conditions such as **2**, bind with considerably higher affinity to those that are not, such as **1** (compare pK_a s of **1** and **2** in Table 2-3). It was therefore of interest to investigate the influence of pH on the binding of **2** to the SH3 domain.

In order to achieve this aim, the ability of **2** to displace **PRP-1** from the SH3 protein was investigated at three different pH values: pH 6.3, 7.3 and 8.3. This pH range was selected because according to the pK_a value for **2** (7.34⁵³), the range covers each of the scenarios where there is nearly complete protonation of **2** (pH 6.3), a 1:1 ratio of protonated and unprotonated species (pH 7.3) and very little protonation (pH 8.3). Because this experiment was performed while many of the preliminary investigations into use of the FP method were underway, the cleaved SH3 protein, as opposed to the GST-SH3 fusion protein was used. Prior to the **PRP-1** displacement experiments, the binding of **PRP-1** to the SH3 domain, at the three different pH values was also investigated, and it was discovered that the affinity of **PRP-1** for the SH3 domain was optimal at higher pH (K_d s = 138, 173 and 224 μ M for pH 8.3, 7.3 and 6.3 respectively, no additional data shown).

2-Aminoquinoline **2** was able to compete for binding with **PRP-1** for the SH3 domain with EC_{50} s of 103, 163 and 395 μ M at pH 6.3, 7.3 and 8.3 respectively (Figure 2-6, Table 2-4). Furthermore, comparison of the competition binding isotherms obtained at each of the pH values (Figure 2-6) clearly illustrates that a trend between pH and affinity of the ligand exists, based on the 'left-shift' nature of the curves with decreasing pH. It should be noted however, that, as was discussed earlier (Section 2.3.1), it is preferable to perform peptide competition assays using the GST-SH3 fusion protein instead of the cleaved SH3 domain due to improved signal to noise. Inspection of these isotherms again illustrates this point, particularly at pH 6.3 where quite large error bars are observed. Thus, there is some uncertainty in the actual EC_{50} values that have been calculated here. Despite this, the

relationship between pH and the affinity of **2** for the SH3 domain is still clear. This provides additional evidence for the importance of protonation on the binding of **2** to the SH3 domain.

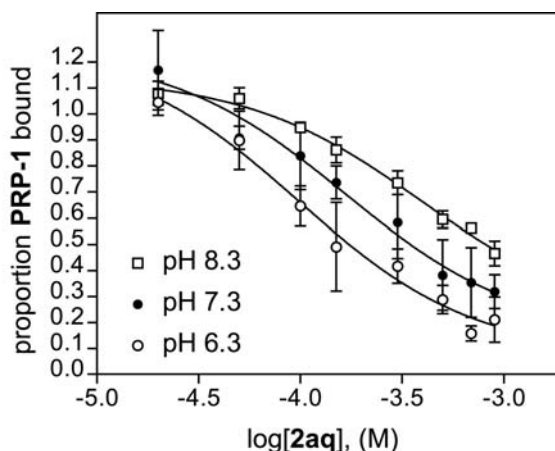


Figure 2-6: Investigation into the effect pH on the affinity of **2** for the Tec SH3 domain as determined by FP peptide displacement experiments, with fluorescently labelled proline-rich peptide **PRP-1**. Overlays of isotherms obtained from independent experiments for competition of **PRP-1** from the cleaved SH3 protein by **2** at pH 6.3, 7.3 and 8.3.

Table 2-4: Effect of pH on the ability of **2** to compete for binding with **PRP-1** for the SH3 domain, as determined by FP peptide displacement assays.

pH	EC ₅₀ (mM) [†]
6.3	103 ± 42
7.3	163 ± 22
8.3	395 ± 18

[†] Quoted values are mean ± standard deviation over three replicate experiments.

2.4.3 Interpretation of SAR information

The above results provide useful SAR information that supplements that obtained from testing of the earlier series of ligands. The observation that 2-aminoquinazoline **1** (which has identical structure to **2** except for the replacement of the carbon at the 3-position of the quinoline ring with an additional nitrogen atom) binds with an approximately six-fold reduction in affinity relative to **2**, can again be rationalised by consideration of the pK_a of **1**. The pK_a of **1** (4.82) (Table 2-3) indicates that there is not a significant level of protonation on the ring nitrogen atom at the pH of the experiment (pH ~ 6.8). The fact that weak binding was still evident when there was a negligible level of protonation, indicates that protonation of the ligand is not essential for binding to occur. However the binding affinity is much enhanced when there is a significant level of protonation on the ligand, leading to formation of a positive

charge (that forms a salt bridge with D196 according to the ligand binding model). Further confirmation of this hypothesis is found on consideration of the effect of pH on the binding of **2** to the SH3 domain: the affinity of **2** was optimal at lower pH. In addition, the EC_{50} obtained for **2** at pH 8.3 was 395 μM , whilst the K_d of **1** at pH 6.7 was 800 μM . The difference in these affinities can be rationalised by calculating the expected level of protonation of the two ligands using their pK_a values and the Henderson-Hasselbach equation. There is approximately 1% protonation of **1** at pH 6.7, but at pH 8.3, there is still approximately 10% protonation of **2**, resulting in higher affinity of **2** under these conditions. It may be predicted then, that if the pH of the experimental conditions was raised even higher, the binding constant of **2** would be closer to that of **1** at lower pH. These results also provide some additional evidence for the involvement of D196 in the ligand binding event.

In the case of compound **19**, which is the single ring equivalent of **1**, binding was abolished altogether. This is consistent with the observation that the single ring equivalent of 2-aminoquinoline **2**, 2-aminopyridine **4**, bound the SH3 domain weakly (K_d **4** > 4000 μM) when there was substantial protonation of both ligands. However, a large decrease in affinity resulted from removal of the second ring (Section 1.4), a consequence of a smaller surface area available for hydrophobic contact with tryptophan 215 (W215). In the present case, loss of the second ring as in **19**, in conjunction with no significant protonation (pK_a of **19** = 3.54) results in complete loss of binding. Using a similar argument, **20** may have also been expected to bind with similar affinity to **1**, but clearly the different size and/or electronic nature of this heterocycle results in no binding.

The result obtained for the 2-amino-5,6,7,8-tetrahydroquinoline **10** derivative is also of particular interest. The EC_{50} for **10** (480 μM) indicates that this ligand competes for binding with **PRP-1** for the SH3 domain with approximately three-fold reduced affinity relative to **2**. On the other hand, this result indicates that an improvement in affinity was obtained by the addition of the second ring to the molecule, relative to the single ring equivalent of **2**, 2-aminopyridine **4** (K_d > 4000 μM , Section 1.4). Therefore the affinities of the three ligands may be placed in the following order: **2** > **10** >> **4**. This suggests that bicyclic systems are preferable to single ring systems. This makes sense, as **10** has similar lipophilic character to **2** but the second ring of **10** has a different shape. Thus **10** should still be able to be involved in a lipophilic contact with W215, providing an improvement in affinity relative to **4**. But, the results also suggest that, of the bicyclic systems, the compound that has aromaticity in both rings (ie. **2**) is optimal.

The result obtained for ligand **8** (ca. three fold reduction in affinity relative to **2**) requires some discussion. Although the pK_a of this compound is unknown, it is reasonable to assume that it is similar to that of **2** and that the reduction in affinity here is a consequence of substitution on the amino group. It may be hypothesised that the reason for the reduced affinity is because of rotation around the H_2N-C bond. Specifically, when the quinoline ring nitrogen atom is protonated, the resulting positive charge on this nitrogen atom can be stabilised by the amino group as illustrated in Figure 2-7. A consequence of this is that there is significant 'partial double bond' character associated with the H_2N-C bond, and therefore, rotamers exist about this partial double bond (Figure 2-7). In the case of unsubstituted 2-aminoquinoline **2** (Figure 2-7, $R = H$), the two rotamers are chemically equivalent, and therefore both are able to interact favourably with the D196 residue of the SH3 domain according to the ligand binding model. Therefore, both rotamers bind the SH3 domain. But by a similar argument, in the case of the *N*-methylated-2-aminoquinoline derivative **8** (again consider Figure 2-7, $R = Me$), it may be hypothesised that only one of the two rotamers is able to interact favourably with D196 and thus only one rotamer binds to the protein. Depending on the relative population of the two rotamers, a higher concentration of **8** is required to obtain the same level of binding that would otherwise be obtained when there is no substitution on the amino group. Although it may also be hypothesised that formation of a favourable interaction with D196 could be a driving force to favour the preferred rotamer (for ligand binding to occur),

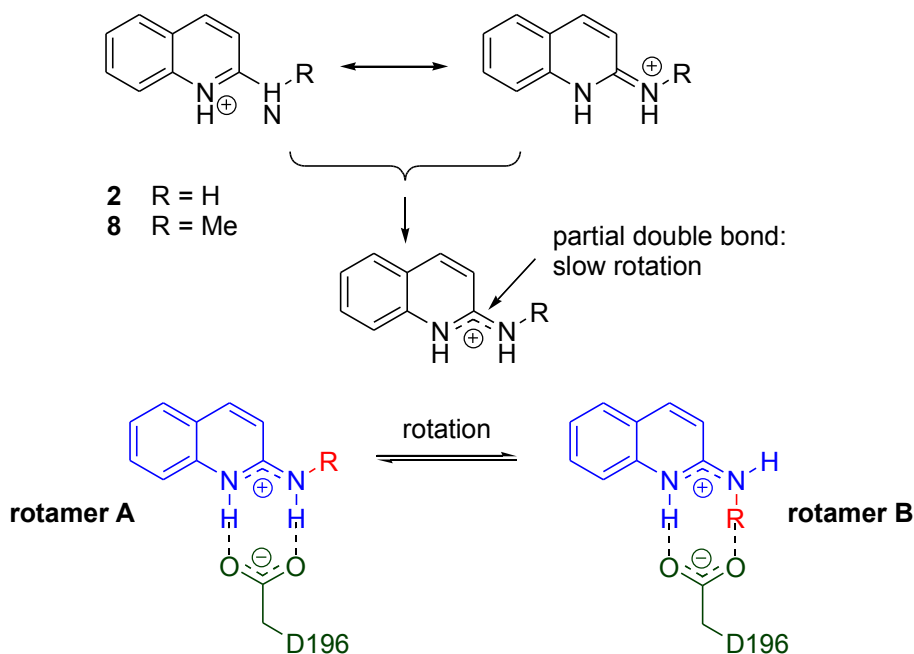


Figure 2-7: Chemical considerations that assist the explanation for why ligand **8** binds the SH3 domain with reduced affinity relative to **2**. Resonance donation from the amino group into the quinoline ring in 2-aminoquinoline **2**, results in slow rotation around the H_2N-C bond. It is therefore possible that only one of the two rotamers (eg when $R = Me$ as in **8**) is able to make a favourable interaction with D196, leading to reduced affinity.

there would be an entropic cost associated with this. This may result in a reduction of the on-rate constant k_{on} for the binding event, and then according to the alternative definition of K_d ($\approx k_{off}/k_{on}$) (see Appendix 1), this leads to a higher K_d value, thereby explaining the reduced affinity observed for ligand **8**.

Careful consideration is also required to assist the explanation for why the *N*-acetyl-2-aminoquinoline derivative **9** did not bind the SH3 domain. Given that **1** was able to bind weakly to the SH3 domain ($K_d = 800 \mu\text{M}$) and the pK_a information indicates that there is no significant protonation on the molecule, it was concluded that protonation of the ligand was not essential, but preferable for binding to occur. In the case of **9**, it is reasonable to assume that the basicity of the quinoline ring nitrogen atom is substantially altered by placement of an acetyl group onto the amino group (because resonance delocalisation can now occur into the carbonyl group as well as into the quinoline ring) and therefore there will be no protonation of the ligand under the experimental conditions. However, since protonation is not essential for binding to occur, **9** may have been expected to bind to the SH3 domain weakly, in a similar fashion to **1**. As no binding was observed for **9**, it may therefore also be concluded in this case that steric and/or other considerations dictate the inability of this compound to bind to the protein. In this situation, it is important to realise that due to resonance considerations, **9** has partial double bond character about the HN-C(quinoline ring) and HN-CO bonds as illustrated in Figure 2-8A, in contrast to **2** which only has partial double bond character about the HN-C(quinoline ring) bond. As a consequence of this, four rotamers of **9** are possible as illustrated in Figure 2-8B below. Because the lone pair of electrons on the acetamido nitrogen atom may be resonance stabilised into either the carbonyl group or the quinoline ring, it may be said that each of the HN-C bonds of **9** is able to rotate more freely than in the case of the HN-C(quinoline ring) bond in **2** (as in Figure 2-7). Of the four structures in Figure 2-8B, only two of them (**9a** and **9b**) are likely to make an electrostatic interaction with D196 as illustrated in Figure 2-8C (for **9a**). The other two structures are likely to become involved in steric clashes or repulsive forces between the oxygen atoms as illustrated in Figure 2-8C (for **9d**). Given that no binding was detected (even at concentrations of **9** as high as 10 molar equivalents of the SH3 domain), suggests that structures **9c** and **9d** (Figure 2-8B) (which are likely to be involved in the steric and/or repulsive clashes) may be the preferred structures of **9**.

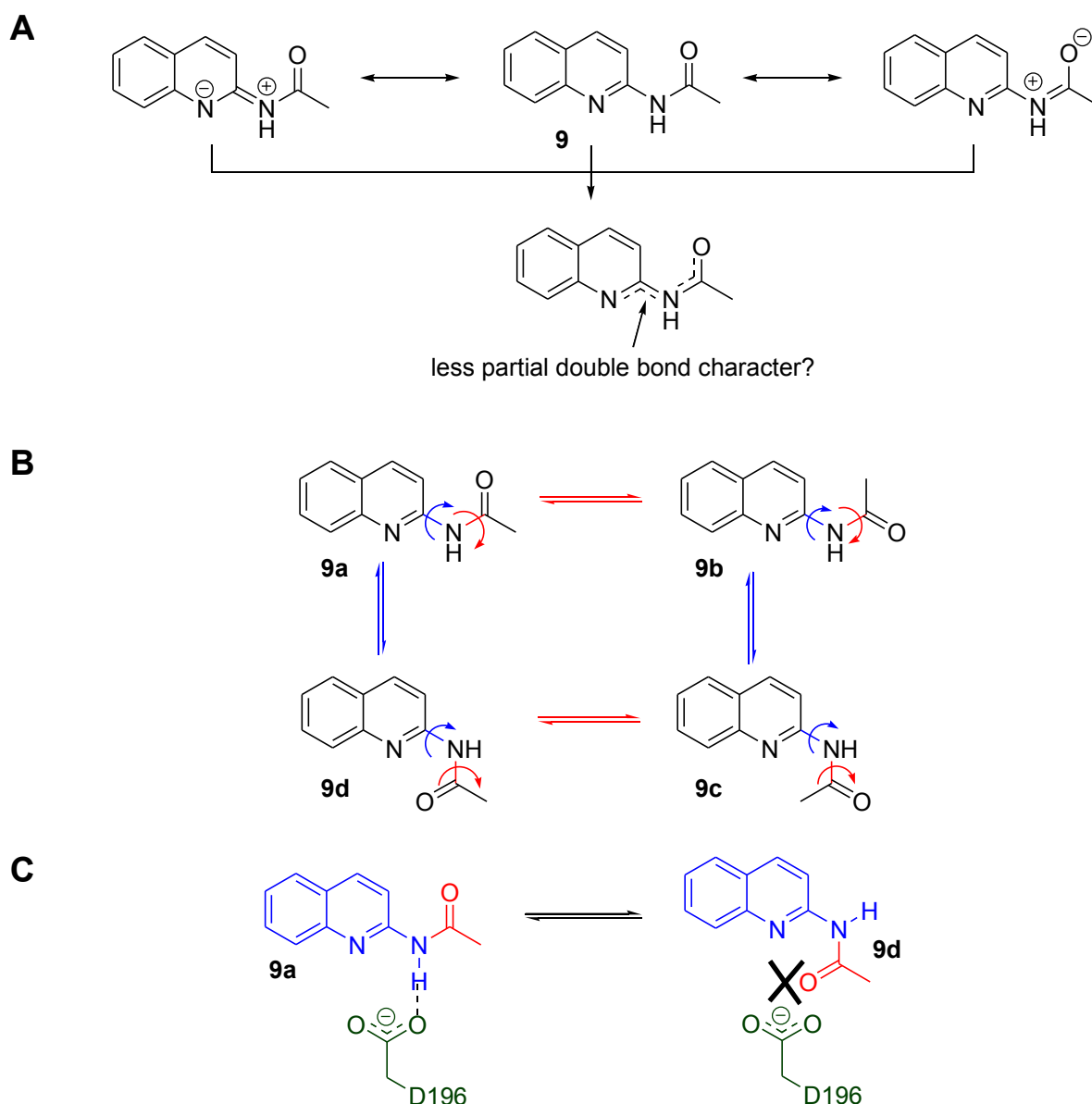


Figure 2-8: Chemical considerations that assist the explanation for why compound **9** does not bind the SH3 domain. (A) Illustration of three different resonance structures of **9**, indicating that both the HN-C(quinoline ring) and HN-CO bonds have partial double bond character. (B) Structures of four possible rotamers of **9** (**9a-d**) resulting from different combinations of rotations around HN-C(quinoline ring) and HN-CO bonds. (C) Illustration of how structure **9a** may make a weak interaction with D196, however **9d** can not, due to repulsion between oxygen atoms.

In the case of the *N*-methyl-*N*-formyl and *N*-diacetyl derivatives **12** and **13**, by a similar argument to that presented above for **9**, it may also be said that the N-C(quinoline ring) bonds may be able to rotate more freely for these compounds, relative to **2**. However this is irrelevant here, given that there are no protons attached to the exocyclic nitrogen atoms (as they both have two substituents attached to the nitrogen). Thus, the same types of electrostatic interactions that allow weak binding of **1** (for example) (that are likely to involve

the NH protons) are not possible in these cases. In addition, steric and/or repulsive clashes (with the *N*-substituents) also explain why these compounds did not bind the SH3 domain.

As for the hydrazinoquinoline derivatives **22** and **23**, the pK_a s of these compounds are unknown. However, it seems chemically reasonable to assume that protonation may occur on either the 'terminal' amino group, or the quinoline ring nitrogen atom, and that a tautomerism equilibrium exists between these two protonated species, as illustrated in Figure 2-9A. However, it is not known in which direction the tautomerism equilibrium lies. Despite

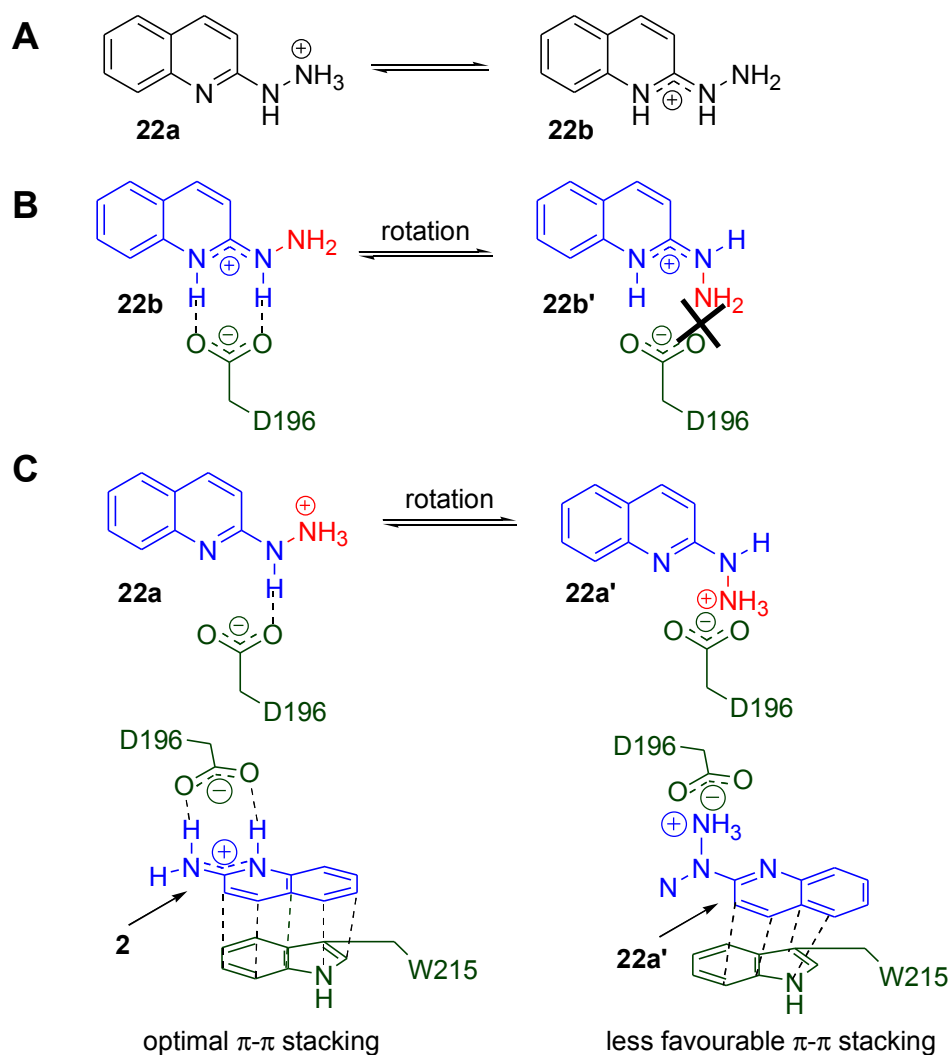


Figure 2-9: Chemical considerations to assist explanation for why hydrazinoquinoline derivatives **22** and **23** bind the SH3 domain weakly. (A) Equilibrium between two tautomers of **22** in the protonated form. (B) Illustration of rotamers of the tautomer **b**, and how only one of these rotamers is likely to make a favourable interaction with D196 of the SH3 domain. (C) Illustration of rotamers of the tautomer **a**: in this situation it is less simple to predict which rotamer would be preferred for ligand binding. In either case, it is likely that the salt bridge formation will have implications on how well the quinoline ring is able to interact with W215. For example as illustrated in the bottom right section, it is proposed that the salt bridge results in very poor π - π stacking with W215, resulting in low affinity, compared to **2** (bottom-left).

this, the low affinity of these ligands may be explained in terms of both tautomers. If tautomer **b** exists, by a similar (rotation) argument to that used for **8** (Figure 2-7), two rotamers exist **22b** and **22b'** (Figure 2-9B). Of these, only **22b** is able to bind the protein as illustrated in Figure 2-9B. Consequently, if the population of tautomer **b** is low, and only a 'sub-population' of this tautomer (rotamer **22b**) is able to bind the protein, this could explain the low affinity.

On the other hand, if tautomer **a** exists, then a salt bridge between D196 and the protonated terminal amino group is likely. But, rotation about the HN-C(quinoline ring) bond once again comes into play, as illustrated in Figure 2-9C. Of the two rotamers **22a** and **22a'**, it is difficult to predict which (if either) is favourable for ligand binding to occur. Despite this, if a salt bridge between D196 and the protonated amino group is formed (for either rotamer **a** or **a'**), then the π - π stacking interaction is likely to be compromised resulting in lower affinity, as illustrated in Figure 2-9C (bottom right portion). This is because, the optimal orientation for the quinoline ring is obtained when the charged atom(s) form part of the HN-C-N(quinoline) system, as for **2** (Figure 2-9C, left). Therefore, to offer an overall explanation for the low affinity of **22**, a combination of all the above factors may need to be considered (tautomerisation and rotation): two or three different species may all bind weakly.

The higher affinity of **22** relative to **23** (K_d s > 1500 and > 3000 μ M respectively) may be a consequence of even less favourable π - π stacking of **23**. A similar argument was used to explain why 2-aminoquinoline **2** binds with approximately six-fold higher affinity than 1-aminoisoquinoline **3** (Section 1.4). In this case, the higher affinity of **2** was attributed to more favourable π - π stacking with W215; for **3**, it was thought that the orientation of the quinoline ring was altered, a consequence of the electrostatic interaction with D196 dictating the orientation of the ring system.⁵¹ In the case of **23**, the π - π stacking is even less favourable than that for **22** (which itself is unfavourable relative to **2**, by a similar argument).

The observation that 2-amino-8-hydroxyquinoline **21** did not bind the SH3 domain provides some evidence for the orientation of the quinoline ring in the ligand binding event. According to the ligand binding model, substituents at the 8-position of the quinoline ring were predicted to not be tolerated, as they would point into the protein surface, and therefore steric violations would result. The result obtained here provides some confirmation of this prediction, and thus support for the proposed orientation of the quinoline ring.

2.4.4 Refinement of 2-aminoquinoline/Tec SH3 domain binding model

The SAR information that was discussed above provides additional support for the proposed ligand binding model, and minimal refinement of the model is required. All of the results can be explained and still fit within the model. An additional five ligands for the SH3 domain with affinities in the range $\sim 400\text{-}3000\ \mu\text{M}$ were identified. Some of the helpful information obtained was the discovery that protonation of the ligand was not essential for binding, but optimal affinity is obtained when there is significant protonation of the pyridyl type nitrogen atom of the ligand. However when only a single ring system is used, protonation of the ligand was essential. These findings suggest that when designing new ligands based on the 2-aminoquinoline scaffold, designs should not lead to significant changes on the pK_a of the quinoline ring nitrogen atom. Indeed, knowledge of the pK_a of a potential ligand would also be of assistance.

The above results also indicate that fused bicyclic ring systems are preferable. However, aromaticity of both rings is not essential, but is desirable. Furthermore, 5-membered rings that contain the pyridyl type nitrogen atom were not tolerated.

Importantly, it was also concluded that optimal affinity ligands are obtained when the amino group is unsubstituted: substitution with a methyl group was tolerated but resulted in an approximately three-fold reduction in affinity. However, substitution with an acetyl group was not tolerated. Substitution with another amino group (as in a hydrazino derivative) resulted in only weak binding.

Despite all these findings, **2** remains the highest affinity compound identified so far, and is therefore the best candidate molecule for development of higher affinity ligands. It is interesting to note that there was some serendipity associated with the discovery of **2** as the highest affinity ligand for Tec SH3 domain binding. 2-Aminoquinazoline **1** was the first compound predicted to bind the SH3 domain, based on the LUDI ligand design, but 2-aminoquinoline **2** was the first compound tested. Compound **2** was first selected based on its structural similarity to **1**, in conjunction with the fact that it was readily available for testing. It turned out to be the highest affinity compound identified following the thorough SAR investigation presented above [in addition to that presented in Chapter 1 (Section 1.4)], but was not 'suggested' as a ligand following the LUDI ligand design. This illustrates the importance of using the results from computational ligand design processes as a guide. Testing of additional compounds with structural similarities to the predicted molecules is of

key importance, in order to maximise the probability of identifying the best possible lead compound.

When [^1H , ^{15}N] HSQC experiments were performed with the D196A mutant SH3 domain (obtained from studies described in Section 1.4) in the presence of **2**, no changes in either ^1H or ^{15}N (HN) chemical shift were observed (data not shown). This not only further confirms the importance of D196 for the binding of **2**, but also confirms single site binding of this ligand. In addition, [^1H , ^{15}N] HSQC experiments with the wild type Tec SH3 domain in the presence of **2** were also performed at reduced temperature, to see if the ligand binding could be driven into slow exchange on the NMR timescale (data not shown). (The relevance of slow exchange ligands was discussed in Sections 1.4 and 1.5.) However, slow exchange binding was not observed.

2.5 Summary: Chapter 2

In this chapter, a range of work was presented, including the synthesis of some simple 2-aminoquinoline derivatives for ligand binding studies, and the testing of these compounds and several others (obtained from various sources) for binding to the Tec SH3 domain. These binding studies provided extra SAR information that was used to assist the understanding of the 2-aminoquinoline **2**/SH3 domain binding event. Of all the compounds tested, no ligands were identified that were higher affinity than **2**, and thus no major revisions of the proposed ligand binding model were made. In addition, the influence of pH on the binding of **2** to the SH3 domain was also investigated, and the importance of protonation of **2** was confirmed. Thus, 2-aminoquinoline **2** remains the best ligand identified so far for development of high affinity ligands for the Tec SH3 domain. Importantly, the results also indicate that optimal affinity ligands will probably best be obtained when there is no substitution on the amino group of **2**.

In addition, investigations concerning important technical considerations for use of Fluorescence Polarisation (FP) as a method of testing for compounds that bind the Tec SH3 domain were also presented in this chapter. These investigations assisted to reveal the optimal conditions for use of the method. Important comparisons between FP and the NMR chemical shift perturbation method were also made. This investigation now paves the way for more effective use of FP as a tool in the current ligand development studies.

Chapter 3

Exploring Methods to Improve 2-Aminoquinoline Binding Affinity 1: Synthesis and Binding Studies of *N*-Benzylated-2-Aminoquinoline Derivatives

3.1 Introduction

The main motivation behind the work presented in Chapter 2 was to continue the characterisation of the 2-aminoquinoline/Tec SH3 domain binding event. Having completed this section of work, and confirming that 2-aminoquinoline was the highest affinity 'lead' compound, it was then time to investigate strategies for the development of 2-aminoquinoline derivatives with improved affinity for the SH3 domain.

To begin this process, regions of the Tec SH3 domain surface that are adjacent to the 2-aminoquinoline binding site according to the ligand binding model were inspected. Regions on the 'left' hand side of where the quinoline ring sits were initially targeted. As illustrated in Figure 3-1, the side chain of phenylalanine 189 (F189) of the SH3 domain was one residue that was initially predicted to be sufficiently close to the ligand binding site, that it may be able to make lipophilic interactions with suitably placed hydrophobic functionality on the ligand. Specifically, ligands with aromatic functional groups may be able to make a π - π stack with F189 (Figure 3-1). As illustrated in Figure 3-1B, when the *N*-benzylated-2-aminoquinoline derivative **24** is manually docked into the 2-aminoquinoline binding site on the SH3 structure (according to the ligand binding model), the distance from the proton at the 4-position of the phenyl ring (of **24**), to the glutamine 190 (Q190) back-bone carbonyl oxygen atom is ca. 2Å. This suggests that a hydrophilic substituent placed on the phenyl ring of **24** is close enough to the Q190 carbonyl oxygen atom, to potentially be involved in hydrogen bonding with Q190.

Thus, in order to explore the protein surface in this region, it was decided to synthesise *N*-benzylated-2-aminoquinolines, as illustrated in Figure 3-1. It should be pointed out however, that this approach may seem 'flawed' on consideration of one of the major conclusions made from interpretation of SAR information in Chapter 2. Specifically, it was concluded that optimal affinity 2-aminoquinoline ligands should be primary amines. This conclusion was drawn based on the fact that the *N*-methylated-2-aminoquinoline **8** bound the SH3 domain with approximately three-fold reduced affinity relative to **2**. But given that larger hydrophobic groups placed in the same region (as the methyl group) may be able to make new contacts with the protein, it was of interest to investigate whether *N*-benzylated

derivatives (eg. **24** in Figure 3-1A) may bind with improved affinity, relative to **8**. Furthermore, it was also anticipated that these compounds would be easy to prepare, by reductive amination of aryl aldehydes with 2-aminoquinoline **2**. Given that many aryl aldehydes with a range of functionality around the aryl nucleus are commercially available, synthesis and binding studies of a series of *N*-benzylated-2-aminoquinolines would potentially be an approach that could provide new SAR information quite quickly.

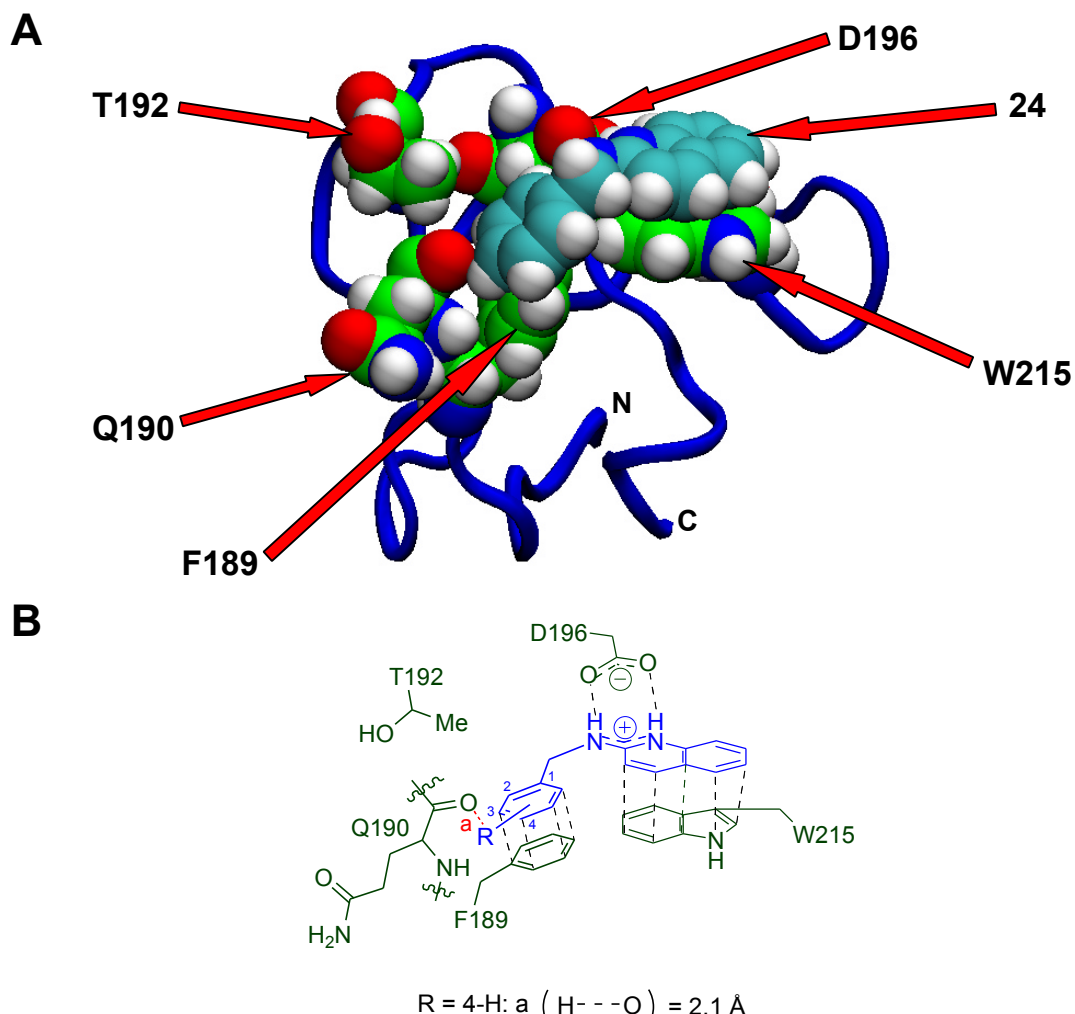
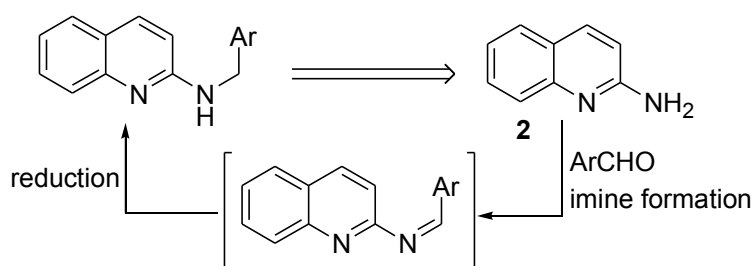


Figure 3-1: Rationale for design of *N*-benzylated-2-aminoquinolines. (A) Regions of amino acids proximal to 2-aminoquinoline on the 'left-hand' side of the binding site, according to the ligand binding model, represented on the published structure of the Tec SH3 domain. The skeletons for amino acid side-chains of the protein are shown in green, and aqua for the ligand, 2-(benzylamino)quinoline **24**. (B) Cartoon representation of regions of amino acids proximal to 2-aminoquinoline on the 'left-hand' side of the binding site, according to the binding model. Protein amino acids are shown in green, and the ligand is shown in blue.

Therefore, the synthesis and SH3 domain binding studies of a small series of *N*-benzylated-2-aminoquinolines is the focus of this Chapter.

3.2 Synthesis of 2-(benzylamino)quinoline derivatives

A widely used approach for the conversion of primary amines to secondary amines is by reductive amination of aldehydes, as illustrated in Scheme 3-1 (using the present targets as an example). This transformation, which occurs via the imine intermediate, may be approached two ways. The amine may be explicitly converted into the imine first. This may typically be done by treatment of the amine with the aldehyde, and heating at reflux in benzene or toluene with a Dean Stark apparatus attached. At the completion of this reaction, the solvent must be removed, before the imine is reduced, using a solvent such as ethanol or methanol. This is effectively a two-step conversion. Alternatively, the imine may be formed and subsequently reduced in a 'one-pot' approach. With the one pot approach, mild forms of hydride, such as sodium cyanoborohydride or sodium triacetoxyborohydride are usually used, so that conversion of the aldehyde to the alcohol prior to imine formation is avoided. Provided that the amine is sufficiently reactive to form the desired imine under relatively mild reducing conditions, then the one pot approach is more efficient. Given that the synthesis of several *N*-benzylated-2-aminoquinolines was planned, it was preferable to identify a method that avoided the need to explicitly synthesise the imine each time. Thus a 'one-pot' method for the conversion of 2-aminoquinoline into *N*-benzylated-2-aminoquinolines was sought.

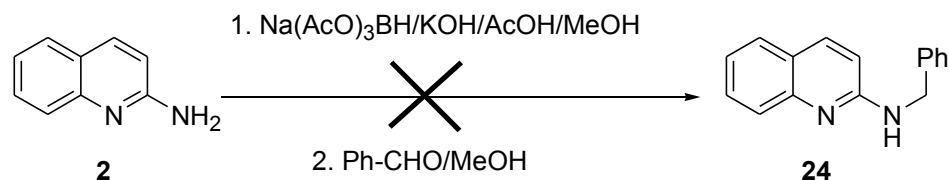


Scheme 3-1: Retrosynthetic plan for the synthesis of *N*-benzylated-2-aminoquinolines, by reductive amination of aryl aldehydes with 2-aminoquinoline **2**.

3.2.1 Investigation into reductive amination using sodium triacetoxyborohydride

This approach was first tested by adaption of a literature procedure involving reductive amination with sodium triacetoxyborohydride using buffered conditions.⁶⁵ 2-Aminoquinoline **2** was treated with benzaldehyde, potassium hydroxide, acetic acid and sodium triacetoxyborohydride in methanol, as illustrated in Scheme 3-2. No reaction between the amine and the aldehyde was observed after several hours at room temperature, as judged by thin layer chromatography. Thus the mixture was heated at ca. 40°C overnight, but again no reaction was observed, as judged by thin layer chromatography and ¹H NMR spectroscopy. Hence it was concluded that the reaction conditions were too mild for

formation of the imine to occur. This is perhaps not surprising given that the paper describing this method was using an aliphatic amine [(*S*)-valine methyl ester], whereas the present study involves an aromatic amine that is resonance stabilised and hence likely to be considerably less nucleophilic than aliphatic amines.

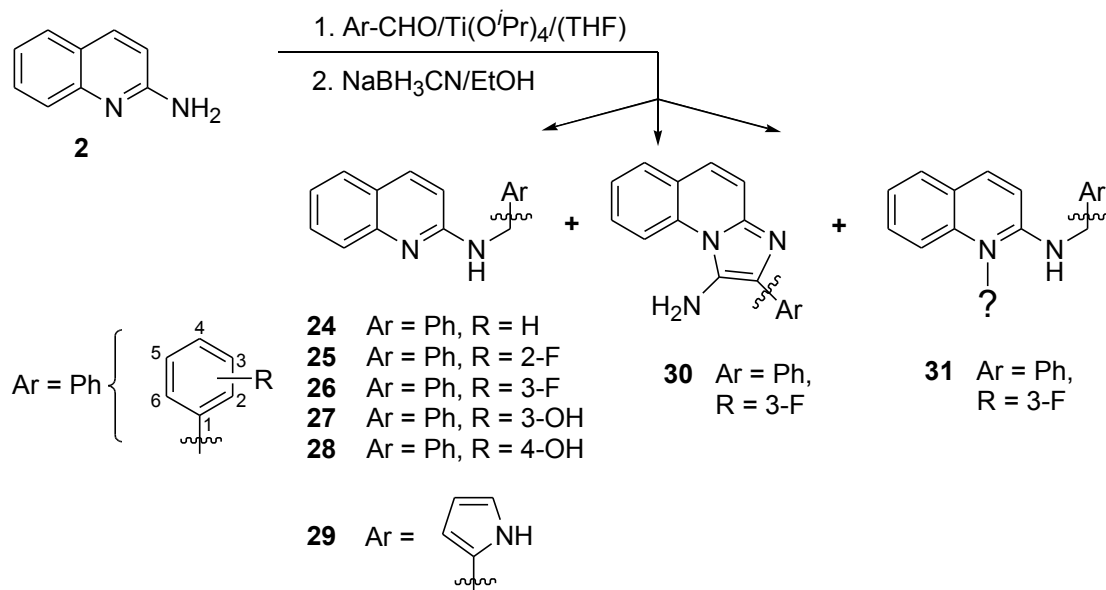


Scheme 3-2: Attempted synthesis of 2-(benzylamino)quinoline **24**, by reductive alkylation of 2-aminoquinoline **2** with benzaldehyde using the method of Manescalchi.⁶⁵

3.2.2 Synthesis of *N*-benzylated-2-aminoquinolines by Lewis acid assisted reductive amination

In order to overcome the apparent low reactivity of 2-aminoquinoline towards imine formation as described above, it was envisaged that reaction conditions involving use of a Lewis acid might be preferable for effecting the desired transformation. Specifically, a 'one-pot' method for the reductive alkylation of a series of mostly aliphatic amines with a range of carbonyl compounds in good to excellent yields, using titanium(IV) isopropoxide has been reported.⁶⁶ This method was therefore tested for suitability for reductive alkylation of 2-aminoquinoline.

2-Aminoquinoline **2** was therefore stirred with benzaldehyde and an excess of titanium(IV) isopropoxide at room temperature overnight as illustrated in Scheme 3-3. After this time, IR spectroscopy suggested that significant consumption of the aldehyde had occurred, as evidenced by the reduction in the size of the band at 1702 cm^{-1} for the carbonyl group of benzaldehyde. Hence, the mixture was diluted with ethanol, and sodium cyanoborohydride was added. The mixture was then stirred for a further 24 hours. Following workup, ^1H NMR spectroscopy of the crude material isolated suggested that the desired product **24** was present as evidenced by a doublet ($J = 4.4\text{ Hz}$) at $\delta \sim 4.70\text{ ppm}$, indicative of the protons at the benzylic position, coupling to the amino proton (CH_2NH). In addition, a broad singlet was observed at $\delta 5.37\text{ ppm}$ suggestive of the proton of the amino group, and a one proton doublet ($J = 9.0\text{ Hz}$) was also observed at $\delta 6.65\text{ ppm}$ as expected for H3 of the quinoline ring. This signal was also shifted slightly upfield (0.07 ppm) relative to the starting material **2** as is expected by alkylation of an amine. However, it was also evident from the ^1H NMR spectrum that at least one other by-product was present in the material.



Scheme 3-3: Method for the synthesis of *N*-benzylated-2-aminoquinoline derivatives **24-29** by titanium(IV) isopropoxide assisted reductive alkylation of 2-aminoquinoline **2** with aryl aldehydes using the method of Mattson.⁶⁶ Formation of the two by-products was observed in each case, however, these products were only characterised in the case of the synthesis of **26**, as indicated above. The structure for the second by-product **31** remains unclear.

Thus the material was chromatographed on a silica gel column, and the pure amine **24** was isolated in 46% yield. The identity of the material was confirmed by mass spectrometry, and the melting point, and ¹H NMR data for **24** were also in good agreement with that presented in the literature. Some additional material of unknown identity was also recovered in approximately 20% mass recovery (based on combined mass of **2** and benzaldehyde). Given the presence of so many signals in the aromatic region of the ¹H NMR spectrum of this material, it was suspected that two products were present. In the first instance, no attempt was made to determine the identity of the product(s) present in this material, because at the time the priority of the work was to prepare *N*-benzylated-2-aminoquinoline derivatives for ligand binding studies with the SH3 domain. Despite the low yield of **24** obtained, it was concluded that this approach would be satisfactory for the synthesis of a series of *N*-benzylated-2-aminoquinolines.

Hence another four derivatives (**25-28**) with varied substitution around the phenyl ring, in addition to **29** where the aryl group was the 5-membered heterocycle pyrrole (joined at the 2-position of the pyrrole ring), were synthesised using essentially the same procedure, as illustrated in Scheme 3-3. In the cases where the starting aldehydes were solids (as for the synthesis of **27-29**), the mixtures were difficult to stir effectively and were frequently inhomogeneous mixtures at the first step of the reaction. To improve the mobility of the mixtures in these cases, a little extra titanium(IV) isopropoxide and/or THF was added. Of

these compounds, the fluorine derivatives **25** and **26** were selected to investigate the influence of strongly electronegative substituents on the affinity of ligand binding. The phenol derivatives **27** and **28** were selected as it was predicted that the hydroxyl group protons might make a hydrogen bond with the carbonyl group of Q190 on the backbone of the SH3 domain as illustrated in Figure 3-1, potentially resulting in a much higher affinity ligand. Compound **29** was selected to investigate the influence on affinity, if any, of an electron-rich 5-membered ring instead of the 6-membered phenyl rings in all the other derivatives.

Table 3-1: Summary of yields for synthesis of *N*-benzylated-2-aminoquinoline derivatives **24-29**, synthesised using the method of Mattson.⁶⁶ (All yields here refer to purified amines, following silica gel chromatography).

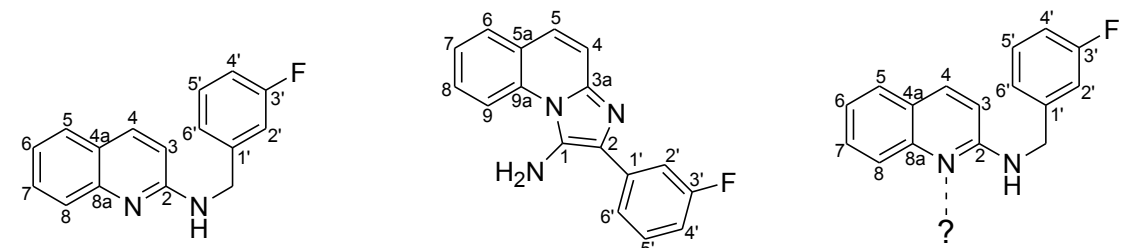
Compound	Yield (%)	Compound	Yield (%)
24	46	27	3
25	23	28	20
26	31	29	28

The yields of the desired amines are summarised in Table 3-1, and were varied, but again were very low to low (3-31%). The features of the ¹H NMR spectrum for the synthesis of **24** described above (δ : ~ 4.5-5 ppm [doublet, $J \sim 5$ Hz, ArCH₂NH], ~ 5-6 ppm [broad singlet, NH] and ~ 6.7 ppm [doublet, $J \sim 9$ Hz, H3 of quinoline ring]) were consistently observed for all the derivatives. In most cases, a complete assignment of all the signals in the ¹H and ¹³C NMR spectra for compounds **25-29** was possible, using a combination of 2D [¹H,¹H] COSY, [¹H,¹H] ROESY, [¹H,¹³C] HMQC and [¹H,¹³C] HMBC experiments. The identities of all the compounds were also confirmed by either elemental analysis, and/or mass spectrometry.

Consistent with the first compound **24** synthesised by this method, two additional by-products were always isolated following column chromatography. The formation of two (not just one) by-products was confirmed in the case of the synthesis of **26**, where two additional pure products were isolated, as judged by ¹H NMR spectroscopy. Each of these two by-products had very distinguishing features in the ¹H NMR spectrum. One of these products gave rise to a doublet ($J \sim 9$ Hz) at ca. δ 9.10 ppm and the other a doublet ($J \sim 9$ Hz) at ca. δ 8.50 ppm. These downfield shifts, which had not been previously observed with any other 2-aminoquinoline derivatives so far, were consistently observed when the ¹H NMR spectra of the by-products were collected for all of the compounds prepared in Scheme 3-3 (although the isolated by-products were not pure in most cases). This suggests that the same two types of by-products were formed in each case. Therefore, the formation of these products contributed to the low yields obtained for the desired amines. Thus, in the case of the synthesis of **26** where each of the two by-products was isolated in a pure form, an effort was

made to determine their identities. As illustrated in Scheme 3-3 and Table 3-2, one of the by-products was determined to be the imidazo[1,2-*a*]quinolin-1-ylamine derivative **30**. Having solved this structure, the yield of **30** could be determined as 10%. The structure of the other by-product **31** remains unclear. However, as illustrated in Scheme 3-3, it is proposed that there is a substituent at the quinoline ring nitrogen atom, but the exact nature of the substituent cannot be determined. This is discussed further later.

There are several pieces of evidence to support the structure **30** as one of the by-products formed in this reaction. At the beginning of this investigation, a compound with molecular mass corresponding to **30** was identified using mass spectrometry. Furthermore, when compared with the structure of the desired product **26**, an additional signal was observed in the ^{13}C NMR spectrum of **30** suggesting there was an additional carbon in the molecule. Given that the reaction involves sodium cyanoborohydride, it was foreseeable that addition of CN at some point was possible. High resolution mass spectrometry confirmed the product had empirical formula $\text{C}_{17}\text{H}_{12}\text{FN}_3$, and this formula indicates that a total of 13 double bonds and/or rings are present in the product. This then suggests that a new ring was formed in the product. A total of 10 signals were observed in the aromatic region of the ^1H NMR spectrum of **30**, and the coupling patterns, in conjunction with connectivities in the COSY spectrum revealed that all three spin systems (H4/H5 and H6-H9 of the quinoline ring, together with the spin system of the 3-fluorophenyl substituent) were intact in this new product. However, the signal at δ 4.74 from the benzylic protons of **26** was not observed in the ^1H NMR spectrum of **30** (Table 3-2). This was accompanied by loss of the benzylic carbon signal at δ 45.9 ppm in the ^{13}C spectrum, and the appearance of a new signal for a quaternary carbon at δ 130.6. Furthermore, this new quaternary signal was a doublet ($J = 2.7$ Hz) consistent with a long range coupling with the fluorine atom of the fluorebenzene motif (Figure 3-2). A broad, two-proton singlet was also present at δ 3.85 in **30**, suggesting that the product was a primary amine, in contrast to **26**. Furthermore, the HMBC spectrum indicated the existence of correlations from the amino protons to the quaternary carbon at δ 130.6 ppm, and another quaternary carbon at δ 129.1, that was previously unaccounted for (Figure 3-2). No other correlations were observed in the HMBC spectrum from this amino group. Hence, the structure **30** was proposed.

Table 3-2: Summary of ^1H and ^{13}C NMR chemical shifts for compounds **26**, **30** and **31**. Note: the structure of second by-product **31** remains unclear.


26			30			31		
Position	δ ^1H (ppm)	δ ^{13}C (ppm)	Position	δ ^1H (ppm)	δ ^{13}C (ppm)	Position	δ ^1H (ppm)	δ ^{13}C (ppm)
2	-	157.1	3a	-	139.8	2	-	156.0
3	6.63	112.0	4	7.34	125.4	3	6.82	109.8
4	7.83	138.3	5	7.41	117.4	4	8.04	143.0
4a	-	124.3	5a	-	124.7	4a	-	123.5
5	7.60	128.1	6	7.73	128.8	5	7.67	129.4
6	7.24	123.1	7	7.40-7.43	124.5	6	7.43	125.3
7	7.55	130.4	8	7.54	127.6	7	7.78	133.4
8	7.71	126.9	9	9.10	116.2	8	8.50	123.0
8a	-	148.4	9a	-	134.6	8a	-	142.6
CH₂	4.74	45.9	2	-	130.6	CH₂	4.72	47.4
1'	-	142.8	1'	-	136.6	1'	-	139.0
2'	7.13	115.2	2'	7.58	114.0	2'	7.07	114.5
3'	-	163.7	3'	-	163.2	3'	-	163.9
4'	6.96	112.8	4'	7.00	113.8	4'	7.04	116.0
5'	7.30	130.8	5'	7.40-7.43	130.3	5'	7.37	131.7
6'	7.18-7.19	123.8	6'	7.61	122.6	6'	7.16-7.18	122.9
-	-	-	1	-	129.1	1	-	-
NH	5.15	-	NH₂	3.85	-	NH	7.52	-

Comparison of the ^1H and ^{13}C NMR chemical shifts at the respective positions around the quinoline and fluorobenzene rings (Table 3-2) reveals many significant differences between the molecules that may be explained using structure **30**. Firstly, there is a downfield change in chemical shift for the H3 proton of **26** from δ 6.63 ppm to δ 7.34 ppm in **30** (H4). When compared with **26**, this is consistent with the substituent at the 3-position of **30** having lost its resonance electron donating effect to the 4-position, resulting in a less shielded carbon, and hence a downfield change in chemical shift. This is in contrast to the **26** where there is a strong resonance contribution from the amino group at the 2-position to C3, resulting in the more upfield chemical shift. In addition, the large downfield changes in chemical shifts

observed at positions 9, 2' and 6' in **30** (compared with positions 8, 2' and 6' in **26**) may also be explained by an anisotropic de-shielding effect being provided by the imidazole ring in **30**. Another key piece of evidence that helped to confirm the structure **30** was the observation of a through space correlation between an NH₂ proton and H9 of the quinoline ring in the [¹H,¹H] ROESY spectrum (Figure 3-2), indicating that these two protons are less than 5 Å apart. The anisotropic de-shielding effect on H9 may also be enhanced by the sp² character expected in the HN-C1 bond, due to resonance donation of the lone pair of electrons on this amino group into the imidazole ring, hence further explaining why such a downfield chemical shift is observed at H9 (δ 9.10 ppm) (Table 3-2). However, comparison of the ¹H and ¹³C chemical shifts between **26** and **30** at positions 5, 6, 7, 4' and 5' for **26** with the corresponding positions in **30** (positions 6, 7, 8, 4' and 5') (Table 3-2) reveals only small changes in chemical shift at these regions of the molecule, also consistent with structure **30**. Some of the key interactions that assisted in assigning the structure of **30** are illustrated in Figure 3-2.

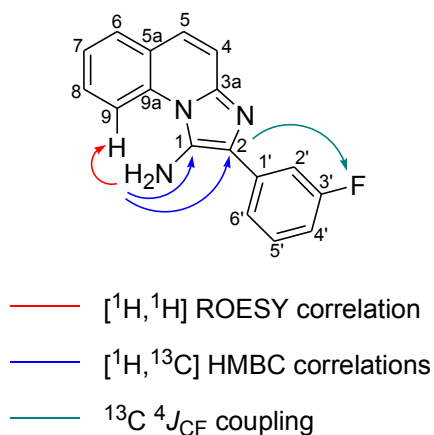


Figure 3-2: Some key interactions observed in NMR experiments that assisted in assigning the structure **30** to one of the by-products formed in the reductive alkylation of 2-aminoquinoline with aryl aldehydes using the method of Mattson.⁶⁶

The formation of structure **30** also makes sense chemically (based on the reagents used for the reaction) and mechanistically. A mechanism for its formation is proposed in Figure 3-3A, involving attack by the carbon atom of cyanide at the benzylic position of the imine intermediate in a Michael sense, resulting in a cyclisation. A subsequent elimination results in formation of the imidazole. Additional support for this structure was found from a report of the synthesis of imidazo[1,2-*a*]quinolin-1-ylamine **32** (lacking the phenyl substituent at the 2-position of the imidazole ring) by treatment of 2-aminoquinoline **2** with formaldehyde and potassium cyanide under mildly basic conditions⁶⁷ (Figure 3-3B). However, no spectral data for **32** was provided in this report for comparison with the data for **30**.

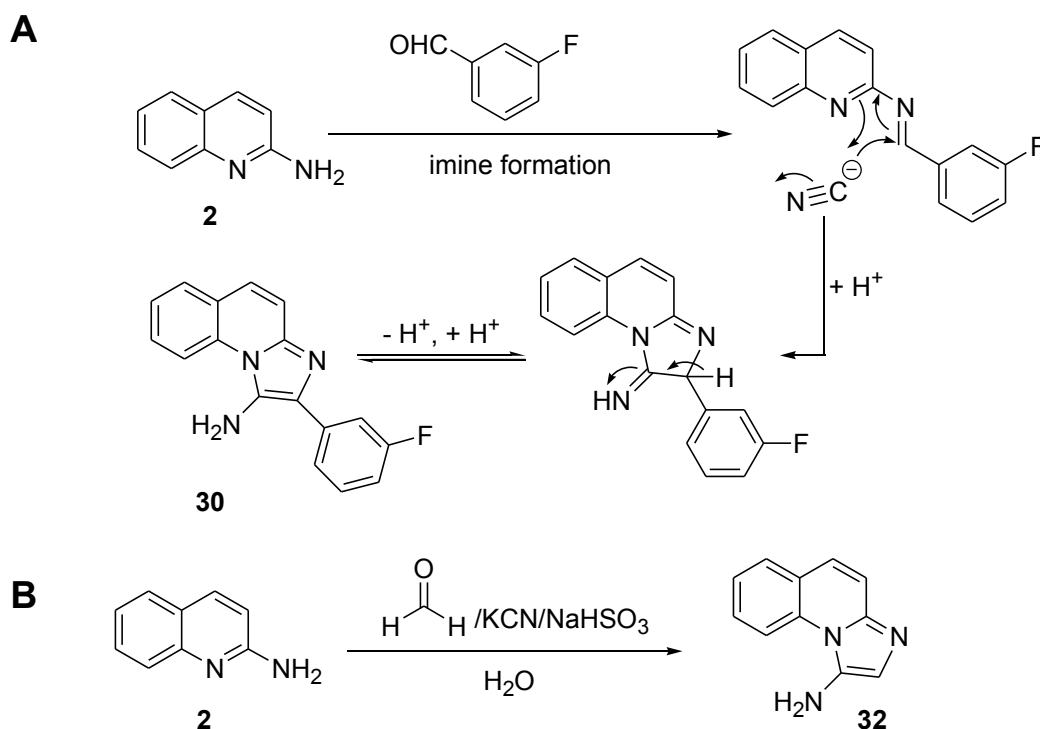


Figure 3-3: (A) Proposed mechanism for the formation of by-product **30** in the reductive amination reaction of 2-aminoquinoline with 3-fluorobenzaldehyde. (B) A reported method⁶⁷ for the synthesis of imidazo[1,2-*a*]quinolin-1-ylamine **32** that lacks substitution at the 2-position of the imidazole ring, using similar reagents to those used for the synthesis of **30**.

On the other hand, some difficulty was experienced when trying to determine the structure of the other unknown by-product **31** formed in the reductive amination reaction. Inspection of Table 3-2 again, reveals there are few substantially altered chemical shifts for **31**, when compared to the desired product **26**. Indeed, the ¹H and ¹³C NMR spectra of **31** reveal the same number of signals in both the aliphatic and aromatic regions are present in both **31** and **26**. Furthermore, as seen in the ¹H NMR spectrum, the benzylic protons remain intact, as evidenced by the doublet at δ 4.72 ppm (ArCH₂NH), and again the [¹H, ¹H] COSY spectrum of **31** confirms the respective connectivities around the quinoline ring are also unaltered. One major difference in the ¹H NMR spectrum of **31** however, was the large downfield change in chemical shift for H8, from δ 7.71 ppm in **26** to 8.50 ppm in **31**. The determination of a structure for this compound was made more difficult given that electron impact mass spectrometry with **31** gave rise to signals corresponding to the molecular masses of **26** and **30**. However, these molecular masses did not seem consistent with the NMR data. However, given the large change in chemical shift observed for H8 in **31**, this suggests that a substituent may be positioned at the quinoline ring nitrogen atom, however, no additional signals were observed in both the ¹H and ¹³C NMR spectra to account for the placement of any additional functionality on the molecule. It was envisaged that **31** may be a quinoline-*N*-oxide derivative, which would explain a downfield chemical change observed for H8 using an

anisotropy argument. However, the existence of an *N*-oxide was not supported by mass spectrometry. Hence, to allow for the possibility that the product was unstable to the electron impact ionisation method, an electrospray (ESI) mass spectrum was obtained. A signal corresponding to the quinoline-*N*-oxide ($m/z = 269$ for $[M+H]^+$) was not observed in the electrospray mass spectrum, but a signal corresponding to a compound of much higher molecular mass than was expected ($m/z = 605$) was observed. In addition a signal was also observed at m/z 314 in the ESI mass spectrum. Again, these signals are not suggestive of any masses that seemed to fit the NMR data for the compound. Thus, no further time was invested in determining the identity of the unknown by-product **31**.

3.3 Ligand binding studies of *N*-benzylated-2-aminoquinoline derivatives with the Tec SH3 Domain

Having synthesised the series of *N*-benzylated-2-aminoquinolines derivatives **24-29** described in the previous section, testing of these compounds for binding to the Tec SH3 domain was then necessary. Given that these compounds are quite hydrophobic, it was envisaged that they would be poorly soluble in buffer alone, and hence they would require the assistance of DMSO to dissolve in aqueous solvent. Therefore the FP method was ruled out as an option for the testing of compounds **24-29**, (for reasons that were discussed in Chapter 2) and the NMR chemical shift perturbation method was instead selected. Indeed, solubility tests confirmed that these compounds were only sparingly soluble in aqueous conditions, even with a 10% DMSO/buffer system (this is discussed more later).

The results of these binding studies, and the interpretation of the new SAR information obtained, is the focus of this Section.

3.3.1 NMR chemical shift perturbation experiments

3.3.1.1 Ligand binding assays

As demonstrated by NMR chemical shift perturbation using $[^1H,^{15}N]$ HSQC NMR experiments, all of the *N*-benzylated-2-aminoquinoline derivatives bound the SH3 domain with approximately one and a half to two-fold reduced affinity relative to **2** (K_d s ca. 180-290 μ M, $K_d = 125 \mu$ M for **2**, Table 3-3) (see for **24** and **27** in Figure 3-4). However, all of these compounds bound with an improvement in affinity relative to **8** ($K_d = 380 \mu$ M) (Table 3-3, Figure 3-4). In the case of ligands **24** and **26**, the improvement was approximately two-fold.

It is important to note however, that under the assay conditions involving the 10% DMSO/buffer system, the maximum concentration possible for compounds **24-29** was ca. 300 μM . Given that the NMR assay typically used a protein sample of concentration $\sim 125 \mu\text{M}$, a maximum of about two-fold concentration of ligand (relative to the protein) was possible for the ligand binding experiments. This is in contrast to the other ligands tested so far that were generally soluble at concentrations of ten to twenty-fold or greater. The consequence of this reduced solubility was that during the ligand binding experiments, it was not possible to reach saturation binding. Thus, the ligand binding isotherms presented in Figure 3-4 are represented as the change in ^1H (H-N) chemical shift observed for the indole side-chain of tryptophan 215 (W215 ϵ 1), instead of the mean of the standardised changes in chemical shift $\{|\Delta\delta/\Delta\delta_{\text{max}}|\}$, determined over all residues where the ^1H (H-N) chemical shift was altered by at least 0.1 ppm, used in Chapters 1 and 2. (In order to make meaningful comparisons between binding isotherms that are standardised, it is essential that saturation binding has been obtained for all ligands compared.) The W215 ϵ 1 ^1H (H-N) signal was selected because this residue forms a key part of the 2-aminoquinoline binding site.

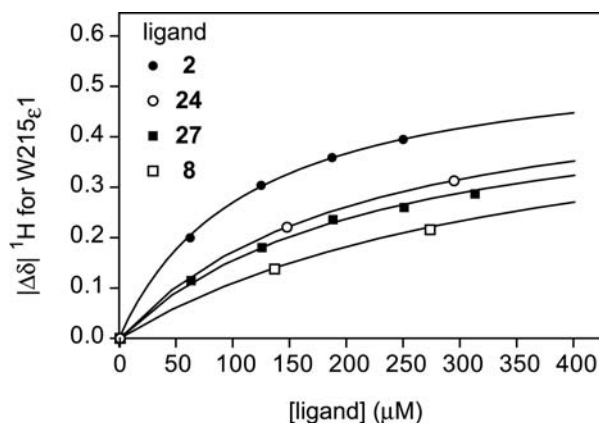
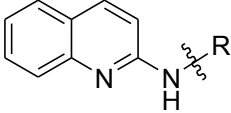
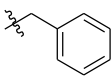
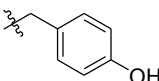
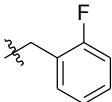
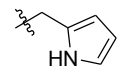
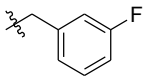
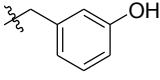


Figure 3-4: Equilibrium binding of *N*-benzylated-2-aminoquinoline derivatives **24** and **27**, and comparison with 2-aminoquinoline **2**, and the *N*-methylated-2-aminoquinoline derivative **8** to the Tec SH3 domain, studied by NMR spectroscopy. Overlays of isotherms, obtained from independent experiments, represented by as change in ^1H (H-N) chemical shift for the indole side-chain (H-N) proton of tryptophan 215 (W215 ϵ 1), a key residue in the 2-aminoquinoline binding site on the SH3 domain.

Table 3-3: Equilibrium binding of *N*-benzylated-2-aminoquinoline derivatives **24-29**, and comparison with the *N*-methylated and unsubstituted compounds **8** and **2**, as determined by NMR spectroscopy.

					
Ligand	R	K_d (mM) [†]	Ligand	R	K_d (mM) [†]
24		193 ± 15	28		292 ± 85
25		208 ± 28	29		285 ± 46
26		177 ± 34	8	Me	380 ± 40
27		234 ± 55	2	H	125 ± 24

[†] Quoted values are mean ± standard deviation over residues whose ¹H (H-N) chemical shift changes were altered by at least 0.1 ppm at the maximum concentration of ligand.

3.3.1.2 Chemical shift mapping of ligand binding events

Mapping the chemical shift changes induced by **24** onto the SH3 fold, and comparison of the mapping for **2** indicates that the two ligands bind at the same location (Figure 3-5 below). Specifically, a similar ‘foot-print’ of chemical shift changes are observed for the two ligands, particularly on the ‘right-hand’ side of, and ‘above’ and ‘below’ the binding site. However, some key differences are noticeable on the ‘left-hand’ side of the binding site as illustrated in Figure 3-5. These features provide some evidence for the new (phenyl) substituent on the 2-aminoquinoline nucleus being positioned on the ‘left-hand’ side, of the ligand binding site, consistent with the predicted binding orientation for the *N*-benzylated-2-aminoquinolines, as illustrated in Figure 3-1. Furthermore, additional evidence for the position of the phenyl group is found on consideration of two chemical shift changes observed on the far left of the fold: the downfield change in ¹H (H-N) chemical shift observed for glutamine 190 (Q190) (yellow region) may be a result of an anisotropic de-shielding effect provided by the ‘edge’ of the phenyl ring, whilst the upfield change for alanine 191 (A191) (red region) may be explained by an anisotropic shielding effect being provided from above the top face of the phenyl ring. It is therefore reasonable to conclude that **24** binds in a similar fashion to that predicted during its design.

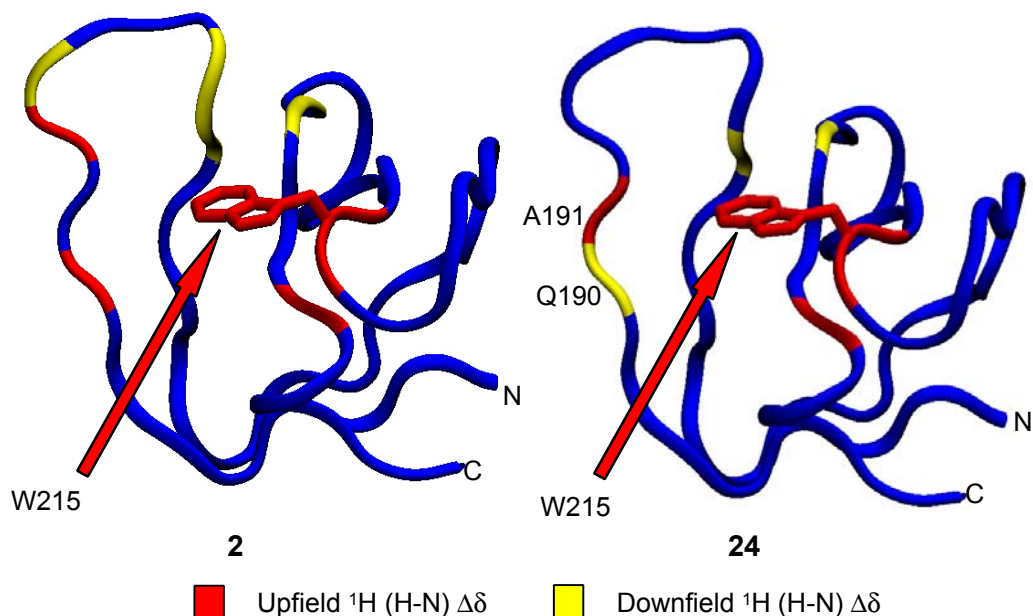


Figure 3-5: Chemical shift mapping of backbone or side-chain (H-N) resonances where δ ^1H (H-N) was altered by at least 0.1 ppm at maximum concentration of ligand **2** (left) and **24** (right).

3.3.2 Discussion of SAR information

The results described above for the binding of the *N*-benzylated-2-aminoquinoline derivatives to the Tec SH3 domain provide new and useful SAR information. Although all of the ligands were lower affinity than 2-aminoquinoline **2**, up to two-fold improved affinity was obtained relative to the *N*-methylated compound **8** (Table 3-3, Figure 3-4). This suggests that a new contact between the SH3 domain and the aryl group of the *N*-benzylated ligands has been formed. Given the proximity of phenylalanine 189 (F189) to the ligand binding site according to the ligand binding model, F189 is the most likely residue to mediate this new interaction, through a lipophilic contact, as predicted in Figure 3-1.

The affinities for the *N*-benzylated-2-aminoquinolines (Table 3-3) were in the range ca. 200-300 μM . Whilst the differences in affinities here are not very significant, these ligands may be placed into 'bins' of approximate affinity. For example, ligands **24-27** may be placed into the $K_d = 200$ μM bin, whilst ligands **28** and **29** could be placed into the $K_d = 300$ μM bin. Using this logic the ligands in the 200 μM bin are of slightly higher affinity than those in the 300 μM bin. These small differences in affinities may be explained in terms of the size and the position of the substituents around the rings. For ligands **24**, **25** and **26** (in the 200 μM bin), there was either no substitution on the phenyl group (**24**), or substitution with small inductively electron withdrawing groups (**25** and **26**), or substitution with relatively larger resonance donating functionality (**27**). But for ligand **28**, the relatively larger (resonance donating) substituent is at the 4-position, and the ligand is in the 300 μM bin. These results

suggest that steric factors may influence the affinity, and that the 2- or 3-position of the phenyl ring is preferable for substitution. The differences in the electronic character of the phenyl groups of ligands **24-27** do not appear to significantly alter the affinity. In the case of ligand **28**, the oxygen atom of the hydroxyl group of **28** may be involved in an electrostatic repulsion with other electronegative atoms on the SH3 domain (eg the carbonyl oxygen atom of Q190 as illustrated in Figure 3-1), contributing to the slightly lower affinity of this ligand. For ligand **29** where the aryl group is the electron-rich 5-membered pyrrole ring, the hydrophobic surface area of the aryl group is reduced in this case. Thus, the lipophilic contact may be slightly weaker, thereby explaining the lower affinity of this ligand.

These results also suggest that the presence of the strongly electronegative fluorine atoms on the phenyl ring (as in ligands **25** and **26**) has minimal influence on the affinity of the ligands. It may also be concluded that the hydroxyl groups on the phenyl ring in the case of ligands **27** and **28** are not involved in 'ideal' hydrogen bonding with any atoms of the SH3 domain, as a much greater improvement in affinity would be expected if this was the case.⁴¹

The above results also provide support for the hypothesis proposed in Chapter 2, for the explanation for why **8** bound the SH3 domain with ca. three-fold reduced affinity relative to **2**. In this hypothesis, it was suggested that rotation around the HN-C (quinoline ring) bond was slow, with two rotamers existing about this 'partial double' bond, and only one of the rotamers was able to bind the protein (when there was an alkyl substituent on the amino group) (see Figure 2-7, Section 2.4.3). Using this argument, the low affinity of **8** can be explained in terms of the population of the two rotamers and/or entropic considerations. Given that the *N*-benzylated ligands described here bind with an improvement in affinity, suggests that entropic contributions to the reduced affinity of **8** can be off-set by substitution with a functional group that is able to make additional contacts with the SH3 domain.

3.4 Summary: Chapter 3

In this Chapter a brief study into the synthesis and binding studies of *N*-benzylated-2-aminoquinolines with the Tec SH3 domain was presented. These compounds were predicted to make hydrophobic and hydrophilic contacts with regions adjacent to the 'left-hand' side of the 2-aminoquinoline binding site, according to the ligand binding model (Figure 3-1).

Six *N*-benzylated compounds were synthesised (**24-29**) by reductive amination of aryl aldehydes with 2-aminoquinoline **2**, by adaption of a literature method.⁶⁶ This method was suitable as a means of obtaining the desired compounds for ligand binding studies, however, the yields were low (< 50%). A contributing factor to the low yields was the formation of two

by-products in the reaction. In the case of the synthesis of *N*-benzylated-2-aminoquinoline derivative **26**, the identity of one of the by-products was determined as the imidazo[1,2-*a*]quinolin-1-ylamine derivative **30** (Scheme 3-3), isolated in 10% yield. An attempt was made to determine the identity of the other by-product, however, conflicting NMR and mass spectrometry data made it difficult to propose a sensible structure for the compound. Ideally, an alternative synthesis for these compounds that avoids the formation of the by-products, leading to higher yields, would be preferable.

The *N*-benzylated compounds synthesised (**24-29**) all bound the Tec SH3 domain with approximately one and a half to two-fold reduced affinity (K_d s ca. 200-300 μ M) relative to 2-aminoquinoline **2** ($K_d = 125 \mu$ M), however, they bound with up to two-fold improved affinity, relative to the *N*-methylated derivative **8**. This suggests that a new contact was made with the SH3 domain. The NMR chemical shift perturbation experiments for **24** suggest that the ligand binds in a fashion similar to that predicted by its design.

However, despite the new and useful SAR information learned from the investigations in this Chapter, 2-aminoquinoline **2** remains the highest affinity ligand identified so far, further confirming that optimal affinity 2-aminoquinoline ligands should be primary amines. So, it would therefore be of interest to investigate the possibility of creating a similar lipophilic contact to that discovered here, via substitution at a different position on the quinoline ring, for example the 3- or 4-position. But in the first instance, development of 3-substituted-2-aminoquinolines was not pursued. Instead, as presented in the following chapter (Chapter 4), the synthesis and binding studies of 6-substituted-2-aminoquinolines was investigated.